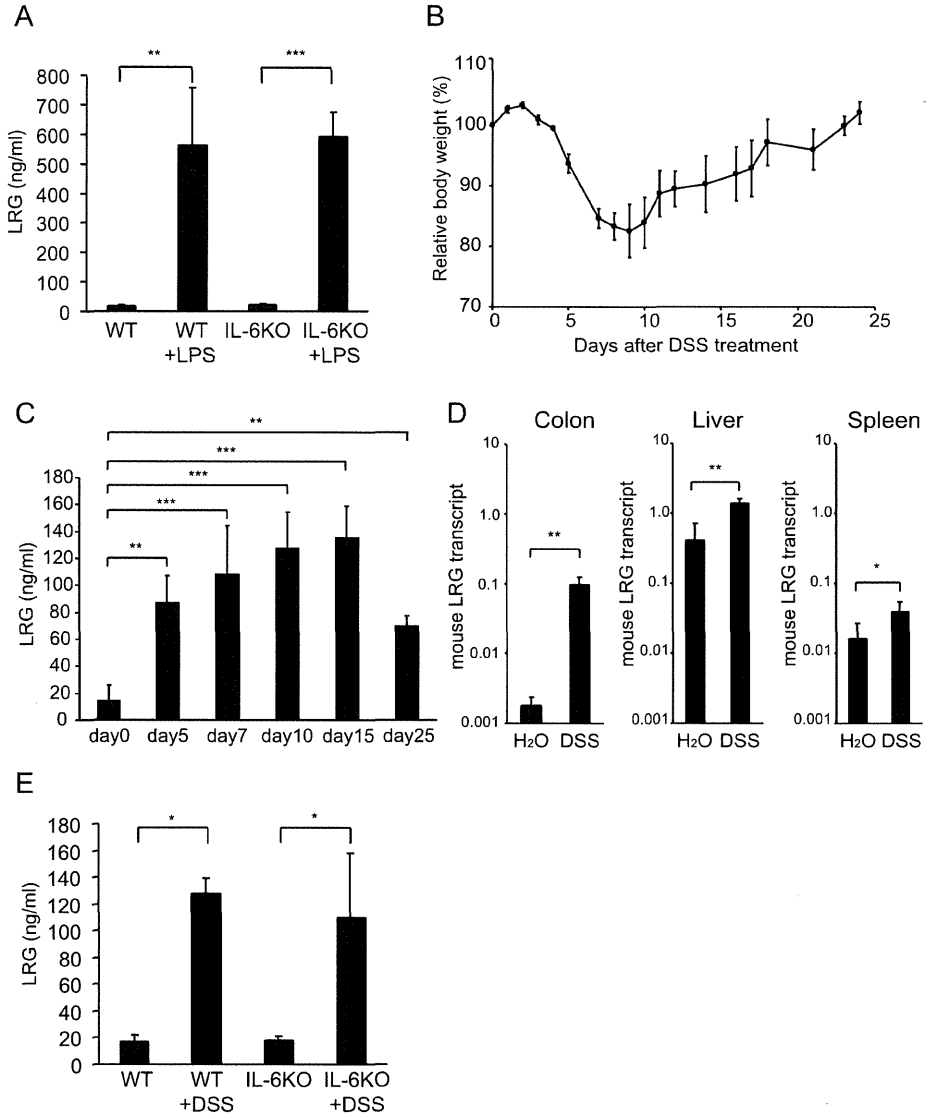

FIGURE 5. Induction of LRG has IL-6-independent pathway in LPS-mediated acute inflammation and active stage of DSS-induced colitis. (A) WT mice and IL-6-deficient mice were injected intraperitoneally with 0 or 10 mg/kg LPS dissolved in 500 μL PBS and serum LRG levels were measured after 24 hours. Data are expressed as mean ± SEM. $^{**}P < 0.005$, $^{***}P < 0.0001$ by one-way ANOVA followed by Scheffe's post-hoc test. (B) Relative body weight changes of mice with DSS-induced colitis in this study. Data are expressed as mean ± SEM ($n = 4$). (C) Expression of LRG is upregulated in murine DSS-induced colitis. At the indicated time, serum LRG levels were determined by ELISA analysis. $^{**}P < 0.005$, $^{***}P < 0.0001$ by one-way ANOVA followed by a by Dunnett's post-hoc test. (D) Nine days after control or DSS treatment, mice were euthanized and gene expression of LRG in the colon, liver, spleen, and kidney was determined by quantitative PCR analysis. Gene expression was calculated relative to HPRT. Data were expressed as mean ± SD ($n = 5$). $^{*}P < 0.05$, $^{**}P < 0.005$ by Student's t-test. (E) IL-6-deficient mice were used for DSS-induced colitis. Nine days after DSS administration, serum levels of mouse LRG was determined by ELISA analysis. $^{*}P < 0.05$ by one-way ANOVA followed by Scheffe's post-hoc test.

however, the strongest induction was observed in colon ($P = 0.000126$).

To investigate whether LRG induction is dependent on IL-6 or not, we analyzed serum LRG levels in IL-6-deficient mice. Interestingly, basal LRG levels in IL-6-deficient mice were similar to those in WT mice and LRG was robustly induced by LPS administration in IL-6-deficient mice (Fig. 5A). Moreover, increased serum LRG levels were also detected in the active stage (day 9) of DSS-induced colitis in IL-6-deficient mice (Fig. 5E). Importantly, the increase of serum LRG in IL-6-deficient mice was similar to that in WT mice (Fig. 5A,E). These findings indicate that LRG expression can be induced in the absence of IL-6.

DISCUSSION

In this study we first demonstrated that serum LRG levels were significantly increased in sera of active UC patients compared with patients in remission and HC. Serum LRG is likely elevated in diverse racial groups, because we detected increased serum LRG levels not only in Japanese patients (Fig. 1A)[13] but also in Caucasian patients with UC (Fig. 1C,D) and CD (data not shown). In addition, levels of serum LRG were significantly correlated with disease activity in UC and the correlation was stronger than CRP. Moreover, by analyzing ROC curve and AUC, serum LRG levels showed higher AUC than CRP and serum LRG levels represented superior sensitivity and specificity to CRP for remission and active of UC by CAI (Fig. 2D), indicating that LRG is a useful marker to evaluate disease activity in UC. In the normal state, serum LRG is thought to be produced from liver and LRG is abundantly found in the sera of HC. In colonic inflammation, we found that the expression of LRG is increased in the inflamed mucosa of UC patients and mice with DSS colitis, suggesting that inflamed tissues can be a source for production of LRG (Fig. 3). The increased expression of LRG in inflamed tissue has previously been observed in appendix during acute appendicitis.[28] Moreover, in acute inflammatory disorders, including appendicitis and diverticulitis, increased expression of serum LRG was observed (Fig. 1A). These results indicate that the elevated expression of LRG at inflamed sites and in sera occurs in various acute and chronic inflammatory disorders. Therefore, increased serum LRG levels are not suitable for use as a specific diagnostic marker of IBD.

CRP is the most common serum marker used to evaluate disease activity in inflammatory diseases. However, serum CRP is primarily dependent on liver production induced by circulating IL-6. Compared with CD and RA, only modest to absent CRP responses are observed in UC, despite active inflammation in colon.[9] Indeed, our cohort of 82 UC patients, analyzed in this study, included five patients with normal value of CRP while having active disease (Fig. 2A). However, our study demonstrated that serum LRG levels were significantly increased in active UC patients' sera and correlated better with disease activity of UC than CRP levels (Figs. 1A, 2A). Particularly, in the group of patients with negative CRP (CRP <0.2), significant correlation was observed between serum LRG levels and CAI (Supporting Fig. 2C). Similarly, among CRP-negative patients serum LRG levels were significantly elevated in those with endoscopically active UC, compared with UC in remission (Supporting Fig. 1B). In addition, serum LRG levels were decreased after therapy (Fig. 2C), suggesting that LRG is a useful serological biomarker for evaluating disease activity and therapeutic effect in UC.

Better correlation of serum LRG levels with disease activity of UC than CRP might be explained in part by the differences in induction mechanisms between LRG and CRP. While the expression of CRP is essentially dependent on IL-6, several cytokines may compensate for the absence of elevated IL-6 in induction of LRG expression. Accordingly, expression of LRG in COLO205 cells was induced not only by IL-6 but also by TNF-α and IL-22 (Fig. 4B), all of which were increased in sera of UC patients (Fig. 4A). Expression of LRG was strongly induced by IL-22 in COLO205 cells, correlating with enhanced STAT3 (Tyr705) phosphorylation by IL-22 compared with IL-6 (data not shown). Thus, inflammatory cytokines such as TNF-α and IL-22 may mediate LRG expression in the absence of IL-6. Moreover, using DSS-induced colitis in IL-6-deficient mice we could demonstrate an IL-6-independent pathway for LRG induction (Fig. 5E). Because promoter regions of human and mouse LRG share high sequence homology and contain putative binding sites for transcription factors such as C/EBP, MZF1, and STAT,[17] it is conceivable that the similar IL-6-independent mechanisms of LRG induction are also involved in humans. Future studies are required to fully elucidate the induction mechanisms of LRG in both humans and mice.

In the three disease categories of UC based on extent of disease, serum LRG levels tended to be low in proctitis compared with extensive colitis and left-sided colitis (Fig. 1B). In addition, correlation between serum LRG levels and disease activity did not reach significance in proctitis (Fig. 2B). Although the low number of patients with active proctitis may preclude the proper evaluation of LRG levels, limited inflamed area of proctitis may also be a reason for slight increases of serum LRG levels in these patients. Given the increased production of LRG in inflamed colonic mucosa, fecal LRG might be a more sensitive disease biomarker for UC including proctitis. Optimization for the measurement of fecal LRG is currently under way in our laboratory.

This study also highlights the potential usefulness of LRG in evaluating murine colitis. Our results indicate that serum LRG levels increase as the disease progresses in a DSS-induced colitis model (Fig. 5B,C). In addition, the LRG expression is significantly upregulated in the colon with DSS-induced colitis (Fig. 5D). Thus, LRG in mice can be an objective disease activity marker for colitis models and may be useful for preclinical studies of IBD.

In conclusion, serum LRG levels reflect disease activity of UC better than CRP, especially in patients with low CRP. In the inflammatory condition, LRG is expressed in the inflamed tissue and expression of LRG is regulated by mechanisms different from that of CRP. These findings suggest that serum LRG is a novel and potential serologic biomarker for evaluating disease activity of UC.

ACKNOWLEDGMENTS

We thank T. Mizushima for provision of appendicitis and diverticulitis patients' sera, Y. Kanazawa for secretarial

assistance, and M. Urase and A. Morimoto for technical assistance.

REFERENCES

1. Nikolaus S, Schreiber S. Diagnostics of inflammatory bowel disease. *Gastroenterology*. 2007;133:1670–1689.
2. Baumgart DC, Sandborn WJ. Inflammatory bowel disease: clinical aspects and established and evolving therapies. *Lancet*. 2007;369: 1641–1657.
3. Stange EF, Travis SP, Vermeire S, et al. European evidence based consensus on the diagnosis and management of Crohn's disease: definitions and diagnosis. *Gut*. 2006;55(Suppl 1):i1–15.
4. Caprilli R, Viscido A, Latella G. Current management of severe ulcerative colitis. *Nat Clin Pract Gastroenterol Hepatol*. 2007;4:92–101.
5. Kornbluth A, Sachar DB. Ulcerative colitis practice guidelines in adults (update): American College of Gastroenterology, Practice Parameters Committee. *Am J Gastroenterol*. 2004;99:1371–1385.
6. Sands BE, Abreu MT, Ferry GD, et al. Design issues and outcomes in IBD clinical trials. *Inflamm Bowel Dis*. 2005;11(Suppl 1):S22–28.
7. Freeman HJ. Use of the Crohn's disease activity index in clinical trials of biological agents. *World J Gastroenterol*. 2008;14:4127–4130.
8. Best WR, Becktel JM, Singleton JW, et al. Development of a Crohn's disease activity index. National Cooperative Crohn's Disease Study. *Gastroenterology*. 1976;70:439–444.
9. Vermeire S, Van Assche G, Rutgeerts P. C-reactive protein as a marker for inflammatory bowel disease. *Inflamm Bowel Dis*. 2004;10: 661–665.
10. Pepys MB, Druguet M, Klass HJ, et al. Immunological studies in inflammatory bowel disease. *Ciba Found Symp* 1977:283–304.
11. Saverymuttu SH, Hodgson HJ, Chadwick VS, et al. Differing acute phase responses in Crohn's disease and ulcerative colitis. *Gut*. 1986; 27:809–813.
12. Colombel JF, Rutgeerts P, Reinisch W, et al. Early mucosal healing with infliximab is associated with improved long-term clinical outcomes in ulcerative colitis. *Gastroenterology*. 2011;141:1194–1201.
13. Serada S, Fujimoto M, Ogata A, et al. iTRAQ-based proteomic identification of leucine-rich alpha-2 glycoprotein as a novel inflammatory biomarker in autoimmune diseases. *Ann Rheum Dis*. 2010;69:770–774.
14. Haupt H, Baudner S. Isolation and characterization of an unknown, leucine-rich 3.1-S-alpha2-glycoprotein from human serum [author's transl]. *Hoppe Seylers Z Physiol Chem*. 1977;358:639–646.
15. Takahashi N, Takahashi Y, Putnam FW. Periodicity of leucine and tandem repetition of a 24-amino acid segment in the primary structure of leucine-rich alpha 2-glycoprotein of human serum. *Proc Natl Acad Sci U S A*. 1985;82:1906–1910.
16. Shirai R, Hirano F, Ohkura N, et al. Up-regulation of the expression of leucine-rich alpha(2)-glycoprotein in hepatocytes by the mediators of acute-phase response. *Biochem Biophys Res Commun*. 2009;382: 776–769.
17. O'Donnell LC, Druhan LJ, Avalos BR. Molecular characterization and expression analysis of leucine-rich alpha2-glycoprotein, a novel marker of granulocytic differentiation. *J Leukoc Biol*. 2002;72: 478–485.
18. Rachmilewitz D. Coated mesalazine (5-aminosalicylic acid) versus sulphasalazine in the treatment of active ulcerative colitis: a randomised trial. *BMJ*. 1989;298:82–86.
19. Kruis W, Schreiber S, Theuer D, et al. Low dose balsalazide (1.5 g twice daily) and mesalazine (0.5 g three times daily) maintained remission of ulcerative colitis but high dose balsalazide (3.0 g twice daily) was superior in preventing relapses. *Gut*. 2001;49:783–789.
20. Matts SG. The value of rectal biopsy in the diagnosis of ulcerative colitis. *Q J Med*. 1961;30:393–407.
21. Iwahori K, Serada S, Fujimoto M, et al. Overexpression of SOCS3 exhibits preclinical antitumor activity against malignant pleural mesothelioma. *Int J Cancer*. 2011;129:1005–1017.
22. Kim A, Enomoto T, Serada S, et al. Enhanced expression of Annexin A4 in clear cell carcinoma of the ovary and its association with chemoresistance to carboplatin. *Int J Cancer*. 2009;125:2316–2322.
23. Fujimoto M, Nakano M, Terabe F, et al. The influence of excessive IL-6 production in vivo on the development and function of Foxp3+ regulatory T cells. *J Immunol*. 2011;186:32–40.
24. Murch SH, Lamkin VA, Savage MO, et al. Serum concentrations of tumour necrosis factor alpha in childhood chronic inflammatory bowel disease. *Gut*. 1991;32:913–917.
25. Woywodt A, Ludwig D, Neustock P, et al. Mucosal cytokine expression, cellular markers and adhesion molecules in inflammatory bowel disease. *Eur J Gastroenterol Hepatol*. 1999;11:267–276.
26. Andoh A, Zhang Z, Inatomi O, et al. Interleukin-22, a member of the IL-10 subfamily, induces inflammatory responses in colonic subepithelial myofibroblasts. *Gastroenterology*. 2005;129:969–984.
27. Okayasu I, Hatakeyama S, Yamada M, et al. A novel method in the induction of reliable experimental acute and chronic ulcerative colitis in mice. *Gastroenterology*. 1990;98:694–702.
28. Kentsis A, Lin YY, Kurek K, et al. Discovery and validation of urine markers of acute pediatric appendicitis using high-accuracy mass spectrometry. *Ann Emerg Med*. 2010;55:62–70 e4.

IJC
International Journal of Cancer

Antiproliferative effect of SOCS-1 through the suppression of STAT3 and p38 MAPK activation in gastric cancer cells

Yoshihito Souma[1], Toshirou Nishida[2], Satoshi Serada[3], Kota Iwahori[3], Tsuyoshi Takahashi[4], Minoru Fujimoto[3], Barry Ripley[5], Kiyokazu Nakajima[1], Yasuaki Miyazaki[1], Masaki Mori[1], Yuichiro Doki[1], Yoshiki Sawa[1] and Tetsuji Naka[3]

[1] Department of Surgery, Osaka University Graduate School of Medicine, Osaka, Japan
[2] Department of Surgery, Osaka Police Hospital, Osaka, Japan
[3] Laboratory for Immune Signal, National Institute of Biomedical Innovation, Osaka, Japan
[4] Department of Surgery, Osaka General Medical Center, Osaka, Japan
[5] Laboratory of Immune Regulation, Osaka University Graduate School of Frontier Biosciences, Osaka, Japan

Inflammation is a crucial driving force in the development of gastric cancers (GCs). Accordingly, persistent activation of STAT3, a transcription factor pivotal in regulating both inflammation and oncogenesis, is often detected in GC, although its mechanism remains elusive. Suppressor of cytokine signaling-1 (SOCS-1) is a negative regulator of proinflammatory cytokine signaling and *SOCS-1* gene methylation is frequently detected in various cancers including GC. However, the significance of *SOCS-1* methylation in GC cells remains unexplored. Our study is undertaken to evaluate the role of SOCS-1 in GC cell proliferation and its effect on signaling pathways in GC cells. Among five GC cell lines, *SOCS-1* gene was methylated in all cell lines and constitutive STAT3 phosphorylation with elevated endogenous IL-6 production was detected in two cell lines (NUGC-3 and AGS). Unexpectedly, anti-IL-6R antibody inhibited neither cell proliferation nor STAT3 phosphorylation in NUGC-3 and AGS. In contrast, enforced SOCS-1 expression by adenoviral vector (AdSOCS-1) markedly suppressed STAT3 phosphorylation and proliferation of NUGC-3 and AGS cells *in vitro*. Interestingly, the antiproliferative effect of SOCS-1 was attributable not only to the inhibition of STAT3 but also to that of p38 MAPK activity, and chemical inhibitors of JAK/STAT and p38 MAPK signaling effectively suppressed proliferation of these GC cells. Furthermore, treatment with AdSOCS-1 *in vivo* significantly suppressed GC proliferation in a xenograft model. These results suggest that *SOCS-1* gene methylation is a critical step in the development of GC, and enforced expression of SOCS-1 may represent a novel therapeutic approach for the treatment of GC.

Cancer Cell Biology

Gastric cancer (GC) is the second most common cause of cancer deaths worldwide.[1] Recent diagnostic and therapeutic advances have significantly improved prognosis for patients with early GC. However, an effective treatment for patients with advanced GC has not yet been established and prognosis remains poor.[2]

Key words: gastric cancer, suppressor of cytokine signaling, Janus kinase, signal transducer and activator of transcription, p38 mitogen-activated protein kinase

Abbreviations: GC: gastric cancer; IL-6R: interleukin-6 receptor; JAK: Janus kinase; p38 MAPK: p38 mitosis-activated protein kinase; SOCS: suppressor of cytokine signaling; STAT3: signal transducer and activator of transcription 3

Additional Supporting Information may be found in the online version of this article.

Grant sponsor: National Institute of Biomedical Innovation
DOI: 10.1002/ijc.27350
History: Received 12 Apr 2011; Accepted 25 Oct 2011; Online 18 Nov 2011

Correspondence to: Tetsuji Naka, Laboratory for Immune Signal, National Institute of Biomedical Innovation, 7-6-8 Saito-Asagi, Ibaraki, Osaka 567-0085, Japan, Tel.: +81-72-641-9844, Fax: +81-72-641-9837, E-mail: tnaka@nibio.go.jp

It has become evident that inflammatory responses can promote cancer development.[3] An important factor in gastric carcinogenesis is persistent inflammation in gastric epithelium due to infection of *H. pylori*.[4] Critical contributors involved in both inflammation and tumorigenesis are proinflammatory cytokines and their downstream signaling pathways. Indeed, dysregulated activation of the JAK/STAT signaling pathway, the major downstream pathway of cytokines such as IL-6, has been detected in various cancers including GC.[5–10] In particular, constitutive activation of STAT3, an important mediator of both proinflammatory and oncogenic signals of IL-6 family cytokines, is linked to inflammation-associated tumorigenesis[6–8,11] and has been detected in ~30% of primary GC.[12] In addition, activation of other signaling pathways, such as mitogen-activated protein kinase (MAPK) and phosphoinositide 3 kinase (PI3K) pathways, downstream of proinflammatory cytokines are also involved in the progression of GC.[13] However, the mechanisms for dysregulated activation of these signaling pathways in cancer cells are largely unknown.

Under homeostatic conditions, cytokine signaling pathways are tightly controlled by negative regulatory mechanisms. The most representative of these mechanisms is the induction of suppressors of cytokine signaling (SOCS) family

proteins, which act in a feedback loop to inhibit cytokine responses by terminating the activation of the JAK/STAT and other signaling pathways.[14–16] The SOCS family, characterized by a central src homology 2 (SH2) domain and a conserved C-terminus SOCS box, is composed of eight structurally related proteins. Among these, SOCS-1 is known as the most potent negative regulator of proinflammatory cytokine signaling.[17] SOCS-1 interacts with phosphorylated tyrosine residues on proteins such as JAK kinases[18,19] to interfere with the activation of STAT proteins or other signaling intermediates. SOCS-1 also recruits the elongin BC-containing E3 ubiquitin-ligase complex *via* the conserved SOCS box to promote the degradation of target proteins.[20] Studies on SOCS-1 deficient mice have indicated that SOCS-1 is essential for the inhibition of excessive immune responses and also are involved in the suppression of tumor development.[17,21] In accordance with this notion, epigenetic silencing of *SOCS-1* by methylation of the CpG island is detected in human cancers, such as hepatocellular carcinoma (HCC), multiple myeloma and pancreatic ductal neoplasm[22–25] and is implicated in cancer development.

Like other cancers, a variety of epigenetic alterations are involved in the development of GC.[26–30] Two groups have recently reported that transcriptional inactivation of *SOCS-1* gene by hypermethylation is frequently observed in GC cell lines[31] and primary GC samples.[32,33] In particular, Oshimo *et al.* have reported that *SOCS-1* gene hypermethylation is not detectable in normal gastric mucosa but is detected in 44% of primary GC tissues and 12% of corresponding non-neoplastic mucosa and is correlated with the progression and lymph node metastasis of GC.[33] However, it remains to be clarified whether the inactivation of *SOCS-1* gene is truly important for the oncogenesis of GC or which signaling pathways targeted by SOCS-1 are important for GC cell proliferation.

In our study, we demonstrate that SOCS-1 is silenced in GC cell lines and is involved in enhanced STAT3 activation in these cells. We also demonstrate that gene delivery of *SOCS-1* in GC cells has a potent antiproliferative effect *via* the suppression of not only JAK/STAT activation but also inhibition of p38 MAPK signaling pathway. Our results provide new insights into the pathogenesis of GC and may highlight potential molecular targets for therapeutic intervention in patients with GC.

Material and Methods

Cell lines

Four human GC cell lines NUGC3 (JCRB0822), MKN45 (JCRB0254), NUGC4 (JCRB0834) and MKN7 (JCRB1025) were obtained from the Japanese Collection of Research Bioresources (Osaka, Japan), and AGS was purchased from the American Type Culture Collection (ATCC, Manassas, VA). All cell lines were maintained in RPMI 1640 medium supplemented with 10% fetal bovine serum (FBS) (HyClone Laboratories, Logan, UT) and 1% penicillin–streptomycin (Nacalai Tesque, Kyoto, Japan) at 37°C under a humidified atmosphere of 5% CO_2.

Enzyme-linked immunosorbent assay

Cell lines were cultured in six-well plates at a density of 1×10^5 cells per well and incubated in RPMI 1640 containing 1% FCS. The concentrations of IL-6, soluble IL-6 receptor (sIL-6R) in the cell culture supernatant was measured at 48-hr time points using Quantikine enzyme-linked immunosorbent assay (ELISA) kits (R&D Systems, Minneapolis, MN) according to the manufacturer's instructions. The ELISA sensitivities for the detection of IL-6 and sIL-6R, as reported by the manufacturer, were 0.7 and 6.5 pg/ml, respectively.

IL-6 and anti-IL-6R antibody treatment of GC cells

After 24 hr of serum starvation, GC cell lines were treated with 20 ng/ml of recombinant IL-6 (PeproTech, Rocky Hill, NJ) and 20 ng/ml of sIL-6R (R&D Systems) and proteins were extracted 15 min after IL-6 stimulation for further analysis. For antibody treatment, 25 and 50 μg/ml of MRA (humanized monoclonal anti-human IL-6R antibody; Chugai Pharmaceutical Co., Tokyo, Japan) was added to cell culture medium with recombinant 20 ng/ml IL-6 and 20 ng/ml sIL-6R. Purified human IgG (Sigma, St. Louis, MO) was used as control. Cells were then harvested for the determination of the phosphorylation status of STAT3.

Methylation-specific PCR

Bisulfite modification of genomic DNA was carried out as described previously.[22,31,33] The bisulfite-treated DNA was amplified with either a methylation-specific or unmethylation-specific primer set using EpiTect methylation-specific PCR (MSP) Kit (Qiagen, Valencia, CA) according to the manufacturer's instructions. The methylation-specific primer sequences in the exon 1 of *SOCS-1* CpG island were 5′-TC GTTCGTACGTCGATTATC-3′ (forward) and 5′-AAAAAA ATACCCACGAACTCG-3′ (reverse); sequences of corresponding unmethylation-specific primer sequences were 5′-TATTTTGTTTGTATGTTGATTATTG-3′ (forward) and 5′-AAACTCAACACACAACCACTC-3′ (reverse). The length of PCR products were 132 bp for methylated reaction, and 122 bp for the unmethylated reaction. PCR products were resolved in 2.5% agarose gels, stained with ethidium bromide and visualized under UV illumination. To ensure that the PCR primers are specific for the detection of methylated or unmethylated bisulfite converted DNA, completely methylated or unmethylated bisulfite converted DNAs, and untreated, unmethylated genomic DNA (EpiTect control DNA, Qiagen), were used for control experiments.

Real-time PCR analysis

After 12 hr of serum starvation, GC cell lines (NUGC3, AGS, MKN45, NUGC4 and MKN7) and human PBMC were treated with 10 ng/ml of recombinant human IFN-γ (PeproTech, Rocky Hill, NJ) for 15 min. Total RNA was prepared

from cells using an RNeasy Mini Kit (Qiagen) and cDNAs were synthesized from 500 ng of each total RNA preparation using a Quantitect Reverse Transcription Kit (Qiagen), all according to the manufacturers' instructions. The forward and reverse primers were as follows: for human SOCS-1 forward primer, 5′-AGACCCCTTCTCACCTCTTG-3′ and reverse primer, 5′-GCACAGCAGAAAAATAAAGC-3′; for β-actin, 5′-GTGGGGCGCCCCAGGCACCA-3′ and 5′-CTCC TTAATGTCACGCACGATTTC-3′.[34] Primers and cDNA were added to SYBR green premix (Invitrogen), which contained all the reagents required for PCR. The PCR conditions of SOCS-1 consisted of 1 cycle at 95°C for 10 min followed by 40–50 cycles of 96°C for 10 sec, 68°C for 15 sec and 72°C for 15 sec; β-actin cycling conditions consisted of 1 cycle at 95°C for 10 min followed by 40–50 cycles of 96°C for 10 sec, 67°C for 30 sec and 72°C for 30 sec. PCR products were measured continuously using the My IQ™ Single-Color Real-Time Detection System (Bio-Rad Laboratories).

Adenoviral vectors

Replication-defective recombinant adenoviral vector expressing the mouse SOCS-1 gene was provided by Dr. Hiroyuki Mizuguchi (Osaka University, Osaka, Japan), which was constructed by an improved *in vitro* ligation method, as described previously.[35,36] An adenoviral vector expressing the LacZ gene was constructed using similar methods. Expression of these genes was regulated by CMV promoter/enhancer and intron A. The viruses were amplified in 293 cells. Viruses were purified by $CsCl_2$ step gradient ultracentrifugation followed by $CsCl_2$ linear gradient ultracentrifugation. The purified viruses were dialyzed against a solution containing 10 mM Tris-HCl (pH 7.5), 1 mM $MgCl_2$ and 10% glycerol and were stored at −80°C. Viral particle and biological titers were determined by a spectrophotometrical method[37] and by using QuickTiter (Adenovirus Titer Immunoassay Kit, Cell Biolabs, San Diego, CA), respectively. After 24-hr incubation of GC cells in culture medium containing 10% FCS, adenoviral vectors were infected by distributing suspensions onto cells at a multiplicity of infection (MOI) of 10–160. Adenoviral vectors containing the genes for HA-tagged Y705F dominant-negative STAT3 (AddnSTAT3) were kindly provided by Dr. Akihiko Yoshimura (Keio University, Tokyo, Japan).

Western-blotting analysis

Cells and tumor tissues from xenograft model were lysed in RIPA buffer (10 mM Tris-HCl, pH 7.5, 150 mM NaCl, 1% Nonidet P-40, 0.1% sodium deoxycholate, 0.1% SDS, 1× phosphatase inhibitor cocktail (Nacalai Tesque) and 1× protease inhibitor cocktail (Nacalai Tesque) followed by centrifugation (13,200 rpm, 4°C, 15 min), after which the supernatants were stored at −80°C until use. Protein concentrations were determined with the DC Protein Assay kit (Bio-Rad Laboratories), using BSA as the concentration standard. Extracted proteins were used for SDS-PAGE or immunoprecipitation assay. For immunoprecipitation assay, extracted proteins were incubated with primary antibody coupled Protein G-Sepharose (BioVision, Mountain View, CA) for several hours at 4°C with rotating. The samples were washed several times with RIPA buffer, and proteins were extracted using SDS sample buffer (0.125 M Tris-HCl, pH 6.8, 10% 2-mercaptoethanol, 4% SDS, 10% glycerol and 0.004% bromophenol blue). Proteins were resolved using 5–20% gradient SDS-PAGE gels (Wako Pure Chemical Industries, Osaka, Japan) and subsequently transferred to PVDF membranes (Millipore, Bedford, MA). The membranes were blocked with 1% BSA in PBS containing 0.1% Tween 20 (PBST) and incubated with the respective antibodies against different targets. The following antibodies were used: anti-SOCS-1, 1:500 (IBL, Fujioka, Japan), anti-HA (Sigma), anti-phospho-STAT3, 1:1,000 (Cell Signaling Technology, Danvers, MA); anti-STAT3, 1:1,000; anti-GAPDH, 1:2,000 (all from Santa Cruz Biotechnology, Santa Cruz, CA).

Next, the membranes were incubated with horseradish peroxidase-conjugated sheep anti-mouse IgG or horseradish peroxidase-conjugated donkey anti-rabbit IgG (GE Healthcare, Little Chalfont, Buckinghamshire, UK). Finally, the signals were visualized by means of an enhanced chemiluminescence (ECL) reaction system (Perkin-Elmer Life Sciences, Boston, MA).

Cell proliferation assay

NUGC3 and AGS cells were plated in 96-well plates at a density of 5×10^2 cells per well and incubated in RPMI 1640 supplemented with 10% FCS for 24 hr. Then, cells were treated with 2.5 μM (NUGC3) and 5.0 μM (AGS) of JAK inhibitor I (Jak inhibitor; Calbiochem, San Diego, CA), with 10 μM (NUGC3) and 20 μM (AGS) of SB203580 (p38 MAP kinase inhibitor; Calbiochem), MRA (anti-human IL-6R antibody; Chugai Pharmaceutical Co.) and dimethyl sulfoxide (DMSO) or human IgG (Sigma) alone, followed by incubation at 37°C in RPMI 1640 supplemented with 5% FBS. Cell proliferation was evaluated with the WST-8 [2-(2-methoxy-4-nitrophenyl)-3-(4-nitrophenyl)-5-(2,4-disulfophenyl)-2H-tetrazolium, monosodium salt] assay (Cell Counting Kit-SF; Nacalai Tesque, Kyoto, Japan) at indicated period after treatment. The absorption of WST-8 was measured at a wavelength of 450 nm with a reference wavelength of 630 nm using a microplate reader Model 680 (Bio-Rad Laboratories, Hercules, CA). Growth rate was expressed as the percentage of absorbance reading for treated cells *vs.* control cells. Each value is the average ± standard deviation (SD) of triplicate wells.

Measurement of p38 MAP kinase and ERK activation

Kinase assays of p38MAPK were performed using commercial kits (Cell Signaling Technology). Cells were seeded 24 hr before the assay in a 100×100 mm^2 polystyrene nonpyrogenic dish at a density of 5×10^5 cells per dish. Cells were harvested at 48 hr after infection of adenoviral vectors and lysed with buffer (20 mM Tris, pH 7.5, 150 mM NaCl, 1

mM EDTA, 1% Triton X-100, 1 mM Na_3VO_4, 1 mg/ml leupeptin and 1 mM PMSF). Five hundred microliters of cell lysates containing 200 μg total protein were incubated with 20 μL of immobilized phospho-p38MAPK monoclonal antibody for p38MAPK assay. The mixtures were then incubated at 4°C overnight and centrifuged to obtain a cell pellet. The pellet was then washed two times with wash buffer and further two times with a kinase buffer (5 mM Tris, pH 7.5, 10 mM $MgCl_2$, 2 mM DTT and 0.1 mM Na_3VO_4). Kinase reactions were carried out in kinase buffer supplemented with 100 mM ATP and 2 μg activating transcription factor-2 (ATF-2) fusion protein as a substrate for p38MAPK assay. Reactions were performed at 30°C for 30 min and terminated by adding 5× SDS-PAGE sample buffer. Total ATF2 and phosphorylated substrates were analyzed by Western-blotting analysis using phospho-ATF-2 (Cell signaling Technology) antibody for kinase assay of p38MAPK.

Mouse xenograft model

All animal experiments were conducted according to the institutional ethical guidelines for animal experimentation of the National Institute of Biomedical Innovation (Osaka, Japan). Male ICR nu/nu mice, 4–5 weeks of age, were obtained from Charles River Japan (Yokohama, Japan). For subcutaneous xenograft experiments, we injected 2×10^6 cells in a total volume of 100 μL of 1/1 (v/v) PBS/Matrigel (Becton Dickinson, Bedford, MA) in the flank of ICR nu/nu mice. After 1 week when the tumor sizes reached to ~100 mm^3, 2×10^8 plaque-forming units (pfu)/50 μL of AdSOCS1 or AdLacZ was injected intratumorally twice per week. Tumor volumes were determined weekly by measuring in two dimensions, length (L) and width (W), and calculating volume as $(W^2 \times L)/2$.

Statistical analysis

Statistical analyses were performed using the StatView 5.0 software package (Abacus Concepts, Berkeley, CA). One-way ANOVA followed by a Scheffe's test or Mann–Whitney U tests were used to evaluate the significance of differences. In all analyses, $p < 0.05$ was considered statistically significant.

Results

Methylation status of SOCS-1 CpG islands in GC cell lines

Since it was reported that *SOCS-1* gene methylation is frequently observed in primary GC,[33] we initially screened five GC cell lines for methylation of the *SOCS-1* gene. By MSP analysis using primers selected from the CpG islands inside exon 1 of the *SOCS-1* gene, we detected *SOCS-1* methylation in all five (NUGC3, AGS, MKN45, NUGC4 and MKN7) GC cell lines (Fig. 1*a*). By real-time PCR analysis, we also found that these five GC cell lines, but not human PBMC, failed to upregulate *SOCS-1* expression in response to IFN-γ, indicating that transcription of the *SOCS-1* gene is inhibited by gene methylation (Fig. 1*b*).

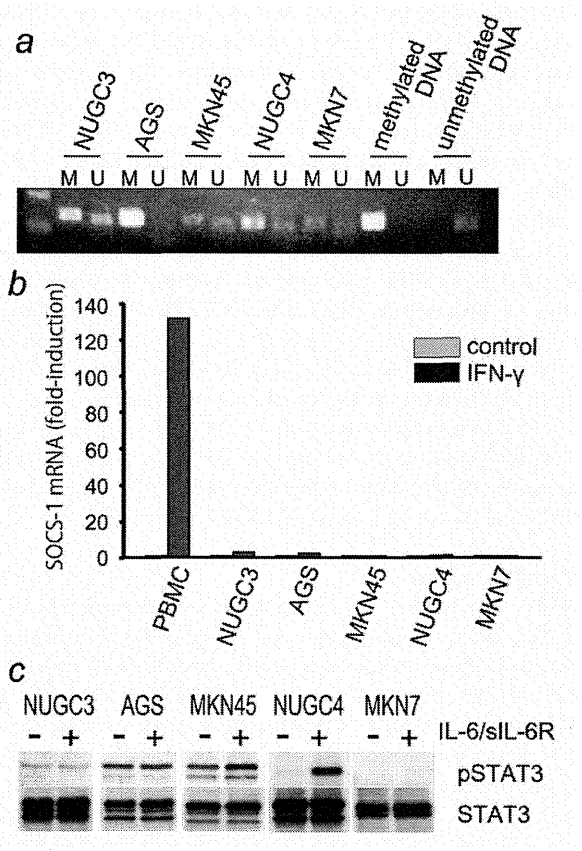

Figure 1. Methylation of *SOCS-1* CpG islands and activation of STAT3 in GC cells. (*a*) MSP of *SOCS-1* gene CpG islands. A visible PCR product in lane-M indicates the presence of methylated gene; the presence of product in lane-U indicates the presence of unmethylated gene. (*b*) Induction of the expression of *SOCS-1* gene with or without stimulation with IFN-γ was analyzed by real-time PCR. (*c*) The phosphorylation of STAT3 was analyzed by Western blotting. Cells were stimulated with 20 ng/ml recombinant IL-6 and 20 μg/ml sIL-6R for 10 min, and protein extracts were subjected to immunoblotting.

Constitutive activation of STAT3 in GC cell lines

We then evaluated the activation status of signal transducer and activator of transcription 3 (STAT3), since STAT3 acts as an important transcriptional mediator of proinflammatory cytokine signaling pathways and contributes to oncogenesis by both preventing apoptosis and enhancing cell proliferation.[11] STAT3 was constitutively phosphorylated in three of five GC cell lines, NUGC3, AGS and MKN45 cells (Fig. 1*c*), raising the possibility that epigenetic silencing of *SOCS* genes may lead to the aberrant activation of the JAK/STAT pathway in these GC cells. In other cell lines, STAT3 phosphorylation was induced strongly in NUGC4 cells after the stimulation with IL-6, but it was not induced in MKN7 cells (Fig. 1*c*).

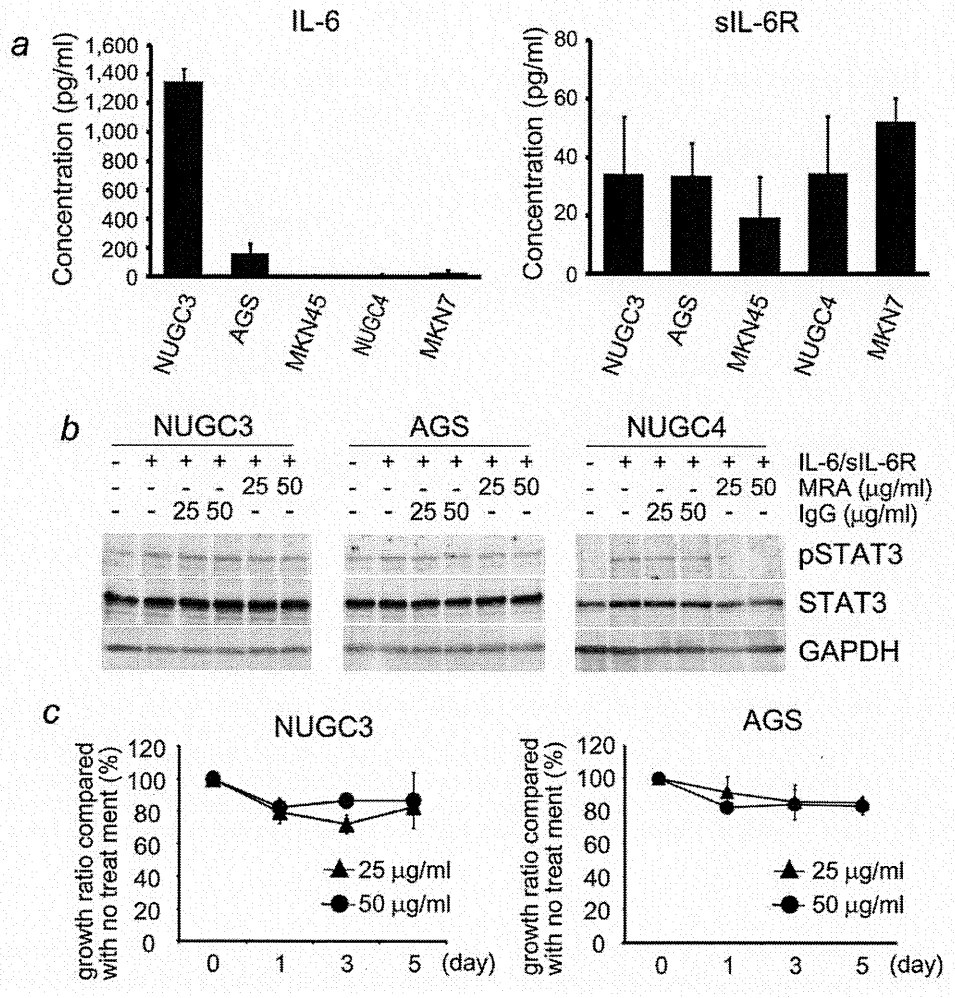

Figure 2. The role of IL-6 production in STAT3 phosphorylation and cell proliferation of GC cells. (*a*) ELISA of IL-6, soluble IL-6 receptor (sIL-6R) protein levels in conditioned media of six GC cell lines. Results are shown as mean ± SD from three independent experiments. (*b*) Effect of anti-IL-6R antibody (MRA) treatment on phosphorylation of STAT3 (Tyr705) was examined by Western-blot analysis in NUGC3, AGS and NUGC4 cell lines. Cell extracts were harvested 15 min after treatment with 20 ng/ml IL-6, 20 μg/ml sIL-6R and 25–50 μg/ml MRA or control IgG, and subjected for immunoblotting with phosphospecific STAT3 (Tyr705) antibody. (*c*) Cell proliferation curves of NUGC3 and AGS cells treated with MRA. Cells were cultured in medium containing 2% FCS with 25 and 50 μg/ml MRA or control human IgG. Cell proliferation was determined by WST-8 assay at 24, 72 and 120 hr after treatment. Percent of cell growth (percent of control) was expressed as mean ± SD value of percentage of absorbance reading from treated cells *vs.* control cells from triplicate wells.

No inhibitory effect of anti-IL-6R antibody on GC cell growth

Previous studies have revealed that IL-6 levels are elevated in cancer tissues[38] and in sera[39,40] of GC patients. We next quantitated levels of IL-6 and soluble IL-6 receptor (sIL-6R) in 48-hr culture supernatants of GC cell lines by sandwich ELISA. As shown in Figure 2*a*, elevated IL-6 levels were observed in NUGC3 cells (1348.6 ± 91.2 pg/ml) and AGS cells (166.3 ± 68.1 pg/ml), while sIL-6R secretion was comparable among all the cell lines tested (Fig. 2*b*). These results suggest that spontaneous production of IL-6 may be crucial for aberrant STAT3 phosphorylation in NUGC3 and AGS cells.

We then assessed the impact of IL-6 blockade on STAT3 phosphorylation and proliferation of NUGC3 and AGS cells, which have demonstrated constitutive STAT3 activation concomitant with high level of IL-6 production (Figs. 1*c* and 2*a*). Western-blot analysis confirmed that humanized anti-IL-6R monoclonal antibody (MRA), which inhibits IL-6 function by competing for the membrane bound and the soluble forms of the human IL-6 receptor,[41] effectively inhibited IL6-induced phosphorylation of STAT3 in NUGC4 cells. However, the

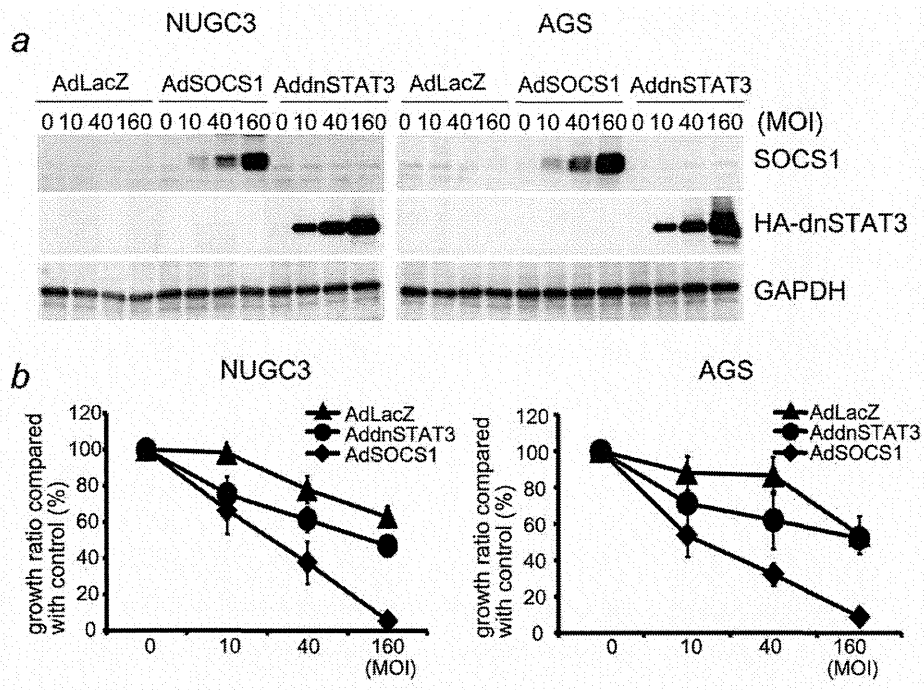

Figure 3. Antiproliferative effect of SOCS-1 in GC cells. (*a*) Western-blot analysis of whole cell extracts to confirm SOCS-1 expression in AdSOCS-1 transfected cells. Cells were infected with AdLacZ, AdSOCS-1 or AddnSTAT3 at an MOI of 10–160. Cell extracts were harvested 24 hr after transfection and subjected for immunoblotting. The expression of SOCS-1 and dnSTAT3 were determined by using anti-SOCS-1 antibody (SOCS-1) and anti-HA antibody (dnSTAT3). (*b*) Cells were infected with AdSOCS-1, AddnSTAT3 or AdLacZ at an MOI of 10–160. Cell proliferation was determined by WST-8 assay at 72 hr after treatment. Growth ratio of AdLacZ-, AdSOCS-1- or AddnSTAT3-infected cells was calculated as the percentage of absorbance reading for infected cells relative to that for nontreated cells. Each value is the average ± SD of triplicate wells.

same treatment could not reduce STAT3 phosphorylation in NUGC3 and AGS cells (Fig. 2*b*). In addition, cell proliferation assay using WST-8 showed that treatment with MRA did not suppress cell proliferation of IL6-producing GC cell lines (Fig. 2*c*). These *in vitro* results suggest that cell proliferation and constitutive STAT3 phosphorylation in NUGC3 and AGS cells occur independently of autocrine IL-6 production, and that signaling pathways other than IL-6 signaling may be involved in cell proliferation of these cells.

Antiproliferative effect of *SOCS-1* gene delivery in GC cells

We next investigated the role of SOCS-1 in regulation of intracellular signaling cascades and GC cell proliferation. For this purpose, we used replication-defective recombinant adenoviral vectors carrying SOCS-1 in cell proliferation assays. Given the established role of STAT3 in tumor development, we also assessed the effect of the inhibition of STAT3-depended pathways, using an adenoviral vector expressing dominant negative STAT3 (dnSTAT3). Immunoblotting analysis showed that adenovirus-mediated gene delivery could induce dose dependent expression of SOCS-1 and dnSTAT3 in both NUGC3 and AGS cells (Fig. 3*a*). As shown in Figure 3*b*, WST-8 assay revealed that adenovirus-mediated *SOCS-1* gene delivery markedly decreased cell proliferation of IL-6 producing NUGC3 and AGS cells. In addition, the magnitude of antiproliferative effects of AdSOCS-1 on GC cells was higher than that of AddnSTAT3. These results suggest that both SOCS-1 and dnSTAT3 can suppress proliferation of NUGC3 and AGS cells, but SOCS-1 is likely to exert additional effects on these GC cells.

Effect of *SOCS-1* gene delivery on JAK/STAT3, MAPK and PI3K pathways

We next determined the activation status of signaling molecules in GC cells infected with AdLacZ, AdSOCS-1 and AddnSTAT3. As shown in Figure 4*a*, immunoblotting analysis showed that phosphorylation levels of STAT3 were effectively decreased in NUGC3 and AGS cells treated with either AdSOCS-1 or AddnSTAT3. Since AdSOCS-1 inhibited GC cell proliferation more effectively than AddnSTAT3, we next investigated if AdSOCS-1 also downregulates STAT3-independent signaling pathway(s) in these cells. Our screening analyses indicated that AKT, SAPK/JNK and p44/p42 MAPK pathways were not affected by AdSOCS-1 infection, although these molecules were constitutively phosphorylated in NUGC3 and AGS cell lines (data not shown). We therefore

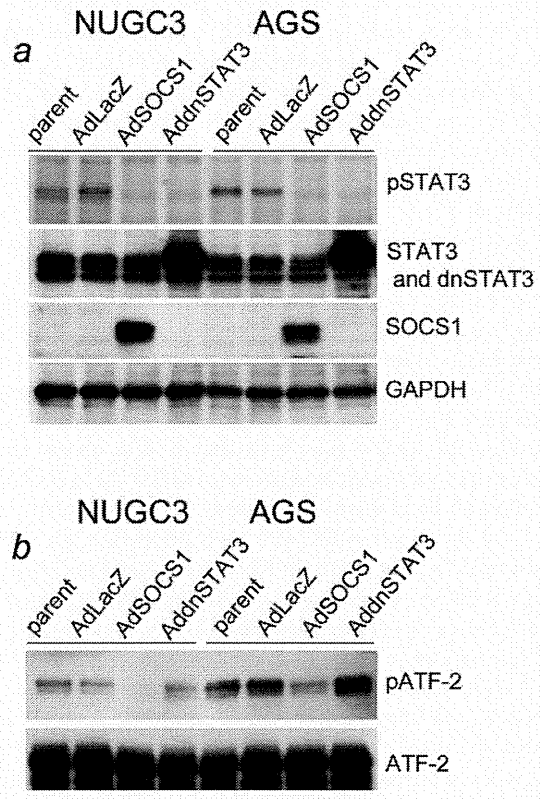

Figure 4. SOCS-1 suppressed the activation of STAT3 and p38 MAPK. (*a*) Cells were infected with AdLacZ, AdSOCS-1 or AddnSTAT3 at an MOI of 40. Cell lysates were prepared at 48 hr after infection, and immunoblotted with SOCS-1, phospho-STAT3 (p-STAT3) and STAT3 antibodies. (*b*) To investigate p38 MAP kinase activity, p38 MAPK was immunoprecipitated and used in an *in vitro* kinase assay with recombinant ATF2 as a substrate. Phosphorylated-ATF2 was determined by immunoblot analysis.

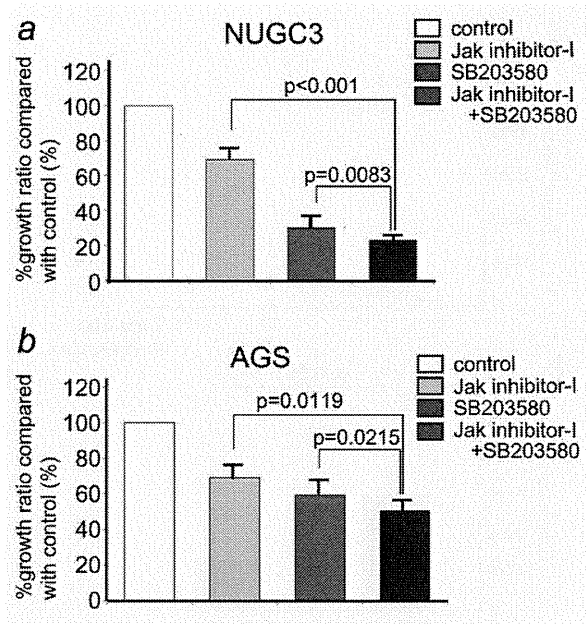

Figure 5. Inhibitors of JAK/STAT and the p38 MAPK signaling pathways suppressed cell growth in GC cells. (*a*) NUGC3 cells and (*b*) AGS cells were cultured in RPMI 1640 medium containing 5% FBS with JAK inhibitor (JAK inhibitor I), with p38 MAPK inhibitor (SB203580) or with JAK inhibitor I and SB203580. Cell proliferation activity was assessed by WST-8-based assay at 72 hr after treatment. Growth ratio (mean ± SD) was calculated as the percentage of absorbance reading for treated cells relative to that for control (DMSO) cells from three independent experiments.

examined another MAPK pathway, the p38MAPK pathway, by evaluating kinase assays with ATF-2 as substrate. Interestingly, the activation of ATF2 in NUGC3 and AGS cells was reduced by AdSOCS-1 infection but not by AddnSTAT3 infection (Fig. 4*b*). Our results indicate that forced expression of SOCS-1 suppresses both JAK/STAT3 and p38 MAPK pathway in NUGC3 and AGS cells.

Inhibition of JAK kinase- and p38 MAP kinase-induced suppression of cell proliferation in GC cells

To confirm whether the activities of JAK/STAT and p38 MAP kinase signaling pathways regulate proliferation of these GC cancer cells, cells were treated with the JAK inhibitor (JAK Inhibitor I), p38 MAP kinase inhibitor (SB203580) or both. Cell proliferation assays revealed that JAK inhibitor I markedly suppressed proliferation in NUGC3 cells (Fig. 5*a*), and moderately suppressed proliferation in AGS cells (Fig. 5*b*). SB203580 suppressed cell proliferation of both NUGC3 and AGS cells more effectively than JAK inhibitor I (Figs. 5*a* and 5*b*). In both NUGC3 and AGS cells, combined treatment with JAK inhibitor I and SB203580 further suppressed the proliferation of these GC cell lines (Figs. 5*a* and 5*b*). Thus, our results suggest that both JAK/STAT3 and p38 MAPK signaling pathways play crucial roles in the proliferation of NUGC3 and AGS cells.

SOCS-1 exhibits antitumor activity in a GC xenograft model

We also evaluated the therapeutic effect of AdSOCS-1 injection on the growth of GC cells *in vivo*. For this purpose, we established a xenograft model of ICR nu/nu mice in which NUGC3 cells were subcutaneously implanted. Injection of AdSOCS-1 vector (1×10^8 pfu/50 μL) intratumorally twice per week suppressed tumor growth compared to tumor volumes in control AdLacZ-injected animals (Figs. 6*a* and 6*b*). AdSOCS-1 *in vivo* could modulate intracellular signaling in GC cells *as in vitro*, since Western-blot analysis showed that phosphorylation levels of STAT3 were decreased in the NUGC3 tissues from AdSOCS-1 injected animals (Fig. 6*c*).

Discussion

Proinflammatory cytokines induced by *H. pylori* infection are critical for both chronic inflammation in gastric mucosa and

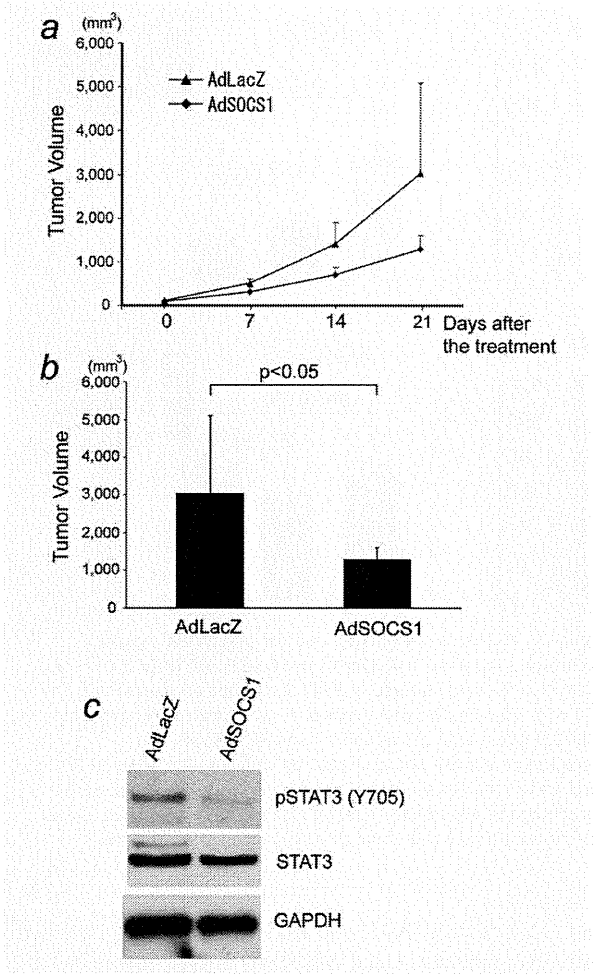

Figure 6. SOCS-1 exhibits antitumor activity in a GC xenograft model. (*a*) Male ICR nu/nu mice, 1 week after the subcutaneous implantation of 2×10^6 NUGC3 cells in their flank, were intratumorally treated with 2×10^8 pfu of AdSOCS1 or AdLacZ twice per week. Tumor volumes were determined weekly. Figures show the average (points) ± SD (bars) for four animals. (*b*) Twenty-eight days after tumor cell inoculation, each tumor volume was calculated. Figures show the average (columns) ± SD (bars) for four animals. (*c*) Western-blot analysis of pSTAT3, STAT3 and GAPDH in NUGC3 tissues from AdSOCS1 or AdLacZ injected animals. NUGC3 tumor-bearing animals were treated once with AdSOCS1 or AdLacZ on day 7 and sacrificed on day 10. Lysates from tumors were analyzed by Western blot.

the initiation and progression of GC. It is thus reasonable to speculate that the changes in sensitivity of gastric epithelial cells to proinflammatory cytokines greatly contribute to the development of GC. In our study, we provide evidence that silencing of *SOCS-1*, a negative regulator of cytokine signaling, is profoundly involved in the development of GC.

We identified *SOCS-1* gene methylation in GC cell lines (Fig. 1*a*). This result is consistent with the previous findings that hypermethylation of the *SOCS-1* gene is detected in GC cell lines and primary GC tissues.[31,33] To *et al.* have previously shown that demethylation treatment can increase SOCS-1 expression and reduce STAT3 activation in GC cell lines.[32] In our study, we demonstrated that forced SOCS-1 expression can inhibit STAT3 activation in GC cells and suppress their proliferation. Our results together with To *et al.* suggest that SOCS-1 functions as a tumor suppressor in GC cells, and its gene silencing should promote GC development and progression.

In our study, we showed that high levels of IL-6 are spontaneously produced in NUGC3 and AGS cell lines. Previous studies have shown that IL-6 facilitates GC cell invasion *in vitro*[42] and serum IL-6 levels correlate well with disease progression and recurrence in GC.[39,40,43] Moreover, the methylation of *SOCS-1* gene is associated with lymph node metastasis and advanced tumor stage in GC.[33] Thus, NUGC3 and AGS cell lines share two features (IL-6 production and *SOCS-1* methylation) of GC with poor prognosis. While the frequency of GC that possesses these two features is currently unknown, future studies on both IL-6-producing capacity and *SOCS-1 gene* methylation status in GC may help to predict the prognosis of GC.

We showed here that STAT3 is persistently activated in several GC cell lines. Similar activation of STAT3 has been reported in other cancer cell lines in which *SOCS-1* gene expression is downregulated by DNA methylation.[22,24,25] One possible mechanism for STAT3 activation in these cells is constitutive production of cytokines such as IL-6. However, in IL-6-producing NUGC3 and AGS cells, anti-IL-6R antibody failed to reduce STAT3 phosphorylation (Fig. 2), suggesting that IL-6 does not act as an autocrine growth factor in these GC cells. Interestingly, conditioned culture media of NUGC3 cells could induce STAT3 phosphorylation in anti-IL-6R antibody-treated human umbilical vein endothelial cells (Supporting Information Fig. 1), suggesting the presence of unknown soluble factor(s) contributing to the STAT3 phosphorylation in NUGC3 cells. However, IL-11, another member of IL-6 family possibly involved in the development of GC,[44] was not elevated in conditioned media of NUGC3 cells (data not shown). These results, nevertheless, suggest that the blockade of IL-6 may have limited therapeutic effects on the growth signals in established GC cells.

In contrast to IL-6 blockade, adenovirus-mediated forced expression of SOCS-1 or dnSTAT3 successfully suppressed cell proliferation of NUGC3 and AGS cells (Fig. 3). The suppressive effect of STAT3 inhibition on GC cell proliferation has been reported previously.[12] Importantly, however, the magnitude of antiproliferative effects of AdSOCS-1 was superior to that of AddnSTAT3, suggesting that AdSOCS-1 has additional mechanism(s) of action distinct from that of AddnSTAT3. Indeed, proliferation of MKN7 cells, in which constitutively phosphorylated STAT3 was not detected (Fig. 1*c*), was successively inhibited by AdSOCS-1, but not by AddnSTAT3 (Supporting Information Fig. 2). Furthermore,

proliferation of MKN45 cells, which exhibited constitutive STAT3 phosphorylation (Fig. 1*c*), was also inhibited by AdSOCS-1 but, surprisingly, not by AddnSTAT3 (Supporting Information Fig. 2). These results indicate that SOCS-1 inhibits not only JAK/STAT3-dependent pathway but also STAT3-independent growth signal pathways. In accordance with this, we found that p38MAPK pathway in GC cells is downregulated by SOCS-1. Moreover, inhibition of these two pathways using JAK inhibitor I and SB203580 had significant antiproliferative effects on GC proliferation. Thus, our results suggest that the potent antiproliferative effect of SOCS-1 is associated with combined inhibition of JAK/STAT3 and p38 MAPK pathways in GC cells.

MAPK family including p38MAPK is activated by a variety of environmental stresses and inflammatory cytokines, and traditionally is thought to play a role in differentiation, growth arrest, inflammation, immune activation and apoptosis. *In vivo*, p38MAPK may function as a tumor suppressor, since mice lacking p38α are sensitized to lung and liver tumors.[45] However, for the development of *H. pylori*-associated GC, p38 MAPK/ATF-2-mediated COX-2 was reported to be necessary.[46] Further studies are needed to elucidate the exact role of p38 MAPK signaling pathway for the growth of GC cells.

In our study, the mechanism by which SOCS-1 suppress the activation of p38 MAPK was not determined. One possible target of SOCS proteins is apoptosis signal-regulating kinase 1 (ASK1), an upstream activator of both the p38 MAPK and JUN N-terminal kinase (JNK) cascades. Supporting this possibility, it has been reported that SOCS-1 regulates the activation of stress-activated MAPKs by binding to ASK1.[47] Moreover, a recent study has shown that ASK1 contributes to tumor growth in GC.[48] SOCS-1 may also target other proteins in GC cells, since SOCS-1 can interact with a variety of tyrosine-phosphorylated proteins *via* their SH2 domain and promote the degradation of target proteins *via* the SOCS box.[21] Recently, we showed that adenoviral gene delivery of SOCS-3, one of the genes of the SOCS family, could inhibit growth of malignant pleural mesothelioma cells *in vitro* and *in vivo via* the modulation of multiple pathways involving JAK/STAT3, ERK, FAK and p53.[41] Although further studies are required, SOCS-1 may also act as an inhibitor of a wide variety of growth signals and may be applicable to the treatment of various types of GC.

In conclusion, we identified *SOCS-1* gene methylation in GC cell lines and highlighted a potent antiproliferative effect of SOCS-1 on GC cells both *in vitro* and *in vivo*, *via* the inhibition of JAK/STAT3 and p38 MAPK activation. Epigenetic silencing of *SOCS-1* may thus represent a critical step in the development of human GC and forced expression of SOCS-1 may represent a novel therapeutic approach for various types of GC through the inhibition of JAK/STAT3 and p38 MAPK signaling pathways.

Acknowledgements

We thank Y. Ito, N. Kawakami and Y. Kanazawa for secretarial assistance, and M. Urase for technical assistance.

References

1. Pisani P, Parkin DM, Ferlay J. Estimates of the worldwide mortality from eighteen major cancers in 1985. Implications for prevention and projections of future burden. *Int J Cancer* 1993; 55:891–903.
2. Dicken BJ, Bigam DL, Cass C, Mackey JR, Joy AA, Hamilton SM. Gastric adenocarcinoma: review and considerations for future directions. *Ann Surg* 2005;241:27–39.
3. Grivennikov SI, Greten FR, Karin M. Immunity, inflammation, and cancer. *Cell* 2010;140:883–99.
4. Peek RM, Jr, Crabtree JE. Helicobacter infection and gastric neoplasia. *J Pathol* 2006;208:233–48.
5. Lacronique V, Boureux A, Valle VD, Poirel H, Quang CT, Mauchauffe M, Berthou C, Lessard M, Berger R, Ghysdael J, Bernard OA. A TEL-JAK2 fusion protein with constitutive kinase activity in human leukemia. *Science* 1997;278: 1309–12.
6. Burke WM, Jin X, Lin HJ, Huang M, Liu R, Reynolds RK, Lin J. Inhibition of constitutively active Stat3 suppresses growth of human ovarian and breast cancer cells. *Oncogene* 2001;20: 7925–34.
7. Bromberg JF, Wrzeszczynska MH, Devgan G, Zhao Y, Pestell RG, Albanese C, Darnell JE, Jr. Stat3 as an oncogene. *Cell* 1999;98:295–303.
8. Rahaman SO, Harbor PC, Chernova O, Barnett GH, Vogelbaum MA, Haque SJ. Inhibition of constitutively active Stat3 suppresses proliferation and induces apoptosis in glioblastoma multiforme cells. *Oncogene* 2002;21:8404–13.
9. Zhang F, Li C, Halfter H, Liu J. Delineating an oncostatin M-activated STAT3 signaling pathway that coordinates the expression of genes involved in cell cycle regulation and extracellular matrix deposition of MCF-7 cells. *Oncogene* 2003;22: 894–905.
10. He B, You L, Uematsu K, Zang K, Xu Z, Lee AY, Costello JF, McCormick F, Jablons DM. SOCS-3 is frequently silenced by hypermethylation and suppresses cell growth in human lung cancer. *Proc Natl Acad Sci USA* 2003;100:14133–8.
11. Yu H, Pardoll D, Jove R. STATs in cancer inflammation and immunity: a leading role for STAT3. *Nat Rev Cancer* 2009;9:798–809.
12. Kanda N, Seno H, Konda Y, Marusawa H, Kanai M, Nakajima T, Kawashima T, Nanakin A, Sawabu T, Uenoyama Y, Sekikawa A, Kawada M, et al. STAT3 is constitutively activated and supports cell survival in association with survivin expression in gastric cancer cells. *Oncogene* 2004; 23:4921–9.
13. Howlett M, Menheniott TR, Judd LM, Giraud AS. Cytokine signalling via gp130 in gastric cancer. *Biochim Biophys Acta* 2009;1793:1623–33.
14. Naka T, Narazaki M, Hirata M, Matsumoto T, Minamoto S, Aono A, Nishimoto N, Kajita T, Taga T, Yoshizaki K, Akira S, Kishimoto T. Structure and function of a new STAT-induced STAT inhibitor. *Nature* 1997;387:924–9.
15. Starr R, Willson TA, Viney EM, Murray LJ, Rayner JR, Jenkins BJ, Gonda TJ, Alexander WS, Metcalf D, Nicola NA, Hilton DJ. A family of cytokine-inducible inhibitors of signalling. *Nature* 1997;387:917–21.
16. Endo TA, Masuhara M, Yokouchi M, Suzuki R, Sakamoto H, Mitsui K, Matsumoto A, Tanimura S, Ohtsubo M, Misawa H, Miyazaki T, Leonor N, et al. A new protein containing an SH2 domain that inhibits JAK kinases. *Nature* 1997;387:921–4.
17. Yoshimura A, Naka T, Kubo M. SOCS proteins, cytokine signalling and immune regulation. *Nat Rev Immunol* 2007;7:454–65.
18. Narazaki M, Fujimoto M, Matsumoto T, Morita Y, Saito H, Kajita T, Yoshizaki K, Naka T, Kishimoto T. Three distinct domains of SSI-1/ SOCS-1/JAB protein are required for its suppression of interleukin 6 signaling. *Proc Natl Acad Sci USA* 1998;95:13130–4.
19. Yasukawa H, Misawa H, Sakamoto H, Masuhara M, Sasaki A, Wakioka T, Ohtsuka S, Imaizumi T, Matsuda T, Ihle JN, Yoshimura A. The JAK-binding protein JAB inhibits Janus tyrosine kinase activity through binding in the activation loop. *EMBO J* 1999;18:1309–20.
20. Krebs DL, Hilton DJ. SOCS proteins: negative regulators of cytokine signaling. *Stem Cells* 2001; 19:378–87.
21. Naka T, Fujimoto M, Tsutsui H, Yoshimura A. Negative regulation of cytokine and TLR signalings by SOCS and others. *Adv Immunol* 2005;87:61–122.
22. Yoshikawa H, Matsubara K, Qian GS, Jackson P, Groopman JD, Manning JE, Harris CC, Herman JG. SOCS-1, a negative regulator of the JAK/

STAT pathway, is silenced by methylation in human hepatocellular carcinoma and shows growth-suppression activity. *Nat Genet* 2001;28: 29–35.
23. Nagai H, Kim YS, Konishi N, Baba M, Kubota T, Yoshimura A, Emi M. Combined hypermethylation and chromosome loss associated with inactivation of SSI-1/SOCS-1/JAB gene in human hepatocellular carcinomas. *Cancer Lett* 2002;186:59–65.
24. Fukushima N, Sato N, Sahin F, Su GH, Hruban RH, Goggins M. Aberrant methylation of suppressor of cytokine signalling-1 (SOCS-1) gene in pancreatic ductal neoplasms. *Br J Cancer* 2003;89:338–43.
25. Galm O, Yoshikawa H, Esteller M, Osieka R, Herman JG. SOCS-1, a negative regulator of cytokine signaling, is frequently silenced by methylation in multiple myeloma. *Blood* 2003; 101:2784–8.
26. Yasui W, Oue N, Kuniyasu H, Ito R, Tahara E, Yokozaki H. Molecular diagnosis of gastric cancer: present and future. *Gastric Cancer* 2001;4: 113–21.
27. Yokozaki H, Yasui W, Tahara E. Genetic and epigenetic changes in stomach cancer. *Int Rev Cytol* 2001;204:49–95.
28. Yasui W, Oue N, Aung PP, Matsumura S, Shutoh M, Nakayama H. Molecular-pathological prognostic factors of gastric cancer: a review. *Gastric Cancer* 2005;8:86–94.
29. Yasui W, Yokozaki H, Fujimoto J, Naka K, Kuniyasu H, Tahara E. Genetic and epigenetic alterations in multistep carcinogenesis of the stomach. *J Gastroenterol* 2000;35 (Suppl 12): 111–5.
30. Yasui W, Oue N, Sentani K, Sakamoto N, Motoshita J. Transcriptome dissection of gastric cancer: identification of novel diagnostic and therapeutic targets from pathology specimens. *Pathol Int* 2009;59:121–36.
31. To KF, Chan MW, Leung WK, Ng EK, Yu J, Bai AH, Lo AW, Chu SH, Tong JH, Lo KW, Sung JJ, Chan FK. Constitutional activation of IL-6-mediated JAK/STAT pathway through hypermethylation of SOCS-1 in human gastric cancer cell line. *Br J Cancer* 2004;91:1335–41.
32. Aihara M, Tsuchimoto D, Takizawa H, Azuma A, Wakebe H, Ohmoto Y, Imagawa K, Kikuchi M, Mukaida N, Matsushima K. Mechanisms involved in Helicobacter pylori-induced interleukin-8 production by a gastric cancer cell line, MKN45. *Infect Immun* 1997;65:3218–24.
33. Oshimo Y, Kuraoka K, Nakayama H, Kitadai Y, Yoshida K, Chayama K, Yasui W. Epigenetic inactivation of SOCS-1 by CpG island hypermethylation in human gastric carcinoma. *Int J Cancer* 2004;112:1003–9.
34. Yamana J, Yamamura M, Okamoto A, Aita T, Iwahashi M, Sunahori K, Makino H. Resistance to IL-10 inhibition of interferon gamma production and expression of suppressor of cytokine signaling 1 in CD4+ T cells from patients with rheumatoid arthritis. *Arthritis Res Ther* 2004;6:R567–77.
35. Mizuguchi H, Kay MA. A simple method for constructing E1- and E1/E4-deleted recombinant adenoviral vectors. *Hum Gene Ther* 1999;10: 2013–7.
36. Sakurai H, Tashiro K, Kawabata K, Yamaguchi T, Sakurai F, Nakagawa S, Mizuguchi H. Adenoviral expression of suppressor of cytokine signaling-1 reduces adenovirus vector-induced innate immune responses. *J Immunol* 2008;180:4931–8.
37. Maizel JV, Jr, White DO, Scharff MD. The polypeptides of adenovirus. I. Evidence for multiple protein components in the virion and a comparison of types 2, 7A, and 12. *Virology* 1968;36:115–25.
38. Yamaoka Y, Kodama T, Kita M, Imanishi J, Kashima K, Graham DY. Relation between cytokines and *Helicobacter pylori* in gastric cancer. *Helicobacter* 2001;6:116–24.
39. Wu CW, Wang SR, Chao MF, Wu TC, Lui WY, P'Eng F K, Chi CW. Serum interleukin-6 levels reflect disease status of gastric cancer. *Am J Gastroenterol* 1996;91:1417–22.
40. Ashizawa T, Okada R, Suzuki Y, Takagi M, Yamazaki T, Sumi T, Aoki T, Ohnuma S. Clinical significance of interleukin-6 (IL-6) in the spread of gastric cancer: role of IL-6 as a prognostic factor. *Gastric Cancer* 2005;8:124–31.
41. Iwahori K, Serada S, Fujimoto M, Nomura S, Osaki T, Lee CM, Mizuguchi H, Takahashi T, Ripley B, Okumura M, Kawase I, Kishimoto T, Naka T. Overexpression of SOCS3 exhibits preclinical antitumor activity against malignant pleural mesothelioma. *Int J Cancer*. 2011;129: 1005-17.
42. Lin MT, Lin BR, Chang CC, Chu CY, Su HJ, Chen ST, Jeng YM, Kuo ML. IL-6 induces AGS gastric cancer cell invasion via activation of the c-Src/RhoA/ROCK signaling pathway. *Int J Cancer* 2007;120:2600–8.
43. Kabir S, Daar GA. Serum levels of interleukin-1, interleukin-6 and tumour necrosis factor-alpha in patients with gastric carcinoma. *Cancer Lett* 1995; 95:207–12.
44. Howlett M, Giraud AS, Lescesen H, Jackson CB, Kalantzis A, van Driel IR, Robb L, van der Hoek M, Ernst M, Minamoto T, Boussioutas A, Oshima H, et al. The interleukin-6 family cytokine interleukin-11 regulates homeostatic epithelial cell turnover and promotes gastric tumor development. *Gastroenterology* 2009;136:967–77.
45. Cuadrado A, Nebreda AR. Mechanisms and functions of p38 MAPK signalling. *Biochem J* 2010;429:403–17.
46. Li Q, Liu N, Shen B, Zhou L, Wang Y, Sun J, Fan Z, Liu RH. Helicobacter pylori enhances cyclooxygenase 2 expression via p38MAPK/ATF-2 signaling pathway in MKN45 cells. *Cancer Lett* 2009;278:97–103.
47. He Y, Zhang W, Zhang R, Zhang H, Min W. SOCS1 inhibits tumor necrosis factor-induced activation of ASK1-JNK inflammatory signaling by mediating ASK1 degradation. *J Biol Chem* 2006;281:5559–66.
48. Hayakawa Y, Hirata Y, Nakagawa H, Sakamoto K, Hikiba Y, Kinoshita H, Nakata W, Takahashi R, Tateishi K, Tada M, Akanuma M, Yoshida H, et al. Apoptosis signal-regulating kinase 1 and cyclin D1 compose a positive feedback loop contributing to tumor growth in gastric cancer. *Proc Natl Acad Sci USA* 2011;108:780–5.

Suppressor of Cytokine Signaling 1 DNA Administration Inhibits Inflammatory and Pathogenic Responses in Autoimmune Myocarditis

Kazuko Tajiri,*,† Kyoko Imanaka-Yoshida,‡,§ Akihiro Matsubara,*,¶ Yusuke Tsujimura,* Michiaki Hiroe,‖ Tetsuji Naka,# Nobutake Shimojo,† Satoshi Sakai,† Kazutaka Aonuma,† and Yasuhiro Yasutomi*,¶

Myocarditis and subsequent dilated cardiomyopathy are major causes of heart failure in young adults. Myocarditis in humans is highly heterogeneous in etiology. Recent studies have indicated that a subgroup of myocarditis patients may benefit from immune-targeted therapies, because autoimmunity plays an important role in myocarditis as well as contributing to the progression to cardiomyopathy and heart failure. Suppressor of cytokine signaling (SOCS) 1 plays a key role in the negative regulation of both TLR- and cytokine receptor-mediated signaling, which is involved in innate immunity and subsequent adaptive immunity. In this study, we investigated the therapeutic effect of SOCS1 DNA administration on experimental autoimmune myocarditis (EAM) in mice. EAM was induced by s.c. immunization with cardiac-specific peptides derived from α myosin H chain in BALB/c mice. In contrast to control myocarditis mice, SOCS1 DNA-injected mice were protected from development of EAM and heart failure. SOCS1 DNA administration was effective for reducing the activation of autoreactive CD4$^+$ T cells by inhibition of the function of Ag-presenting dendritic cells. Our findings suggest that SOCS1 DNA administration has considerable therapeutic potential in individuals with autoimmune myocarditis and dilated cardiomyopathy. ***The Journal of Immunology*****, 2012, 189: 2043–2053.**

Dilated cardiomyopathy (DCM) is a potentially lethal disorder of various etiologies for which no treatment is currently satisfactory (1); it often results from enteroviral myocarditis (2, 3). Many patients show heart-specific autoantibodies (3, 4), and immunosuppressive therapy can improve cardiac function in DCM patients who show no evidence of viral or bacterial genomes in heart biopsy samples (5). These observations suggest that autoimmunity plays an important role in myocarditis as well as contributing to the progression to cardiomyopathy and heart failure (6).

Experimental autoimmune myocarditis (EAM) is a model of postinfectious myocarditis and cardiomyopathy (7). A number of proinflammatory cytokines, including IL-1β, IL-6, IL-12, TNF-α, and GM-CSF, have been shown to contribute to the development of autoimmune myocarditis in animal models and human cases (8–13). EAM is a CD4$^+$ T cell-mediated disease (7, 14), and activation of self-Ag–loaded dendritic cells (DCs) is critical for expansion of autoreactive CD4$^+$ T cells. Activation of TLRs and IL-1 type 1 receptor and their common downstream signaling adaptor molecule, MyD88, in self-Ag–presenting DCs is also critical for the development of EAM (11, 15, 16). Compared with inhibition of a single cytokine, a more effective treatment might be inhibition of various signaling pathways to induce production of cytokines through both innate and adaptive immunity. One strategy that could accomplish this would be to target shared cytokine and TLR signal transduction pathways using suppressor of cytokine signaling (SOCS) molecules.

Recent lines of evidence indicate that SOCS proteins, originally identified as negative-feedback regulators in cytokine signaling, are involved in the regulation of TLR-mediated immune responses (17, 18). The SOCS family is composed of eight members: cytokine-inducible Src homology 2 domain-containing protein and SOCS1 to SOCS7 (19, 20). SOCS1 plays a key role in the negative regulation of both TLR-mediated signaling and cytokine receptor-mediated signaling, which are involved in innate immunity and subsequent adaptive immunity (21). The expression of SOCS1 is induced by various cytokines, including IFN-γ, IL-4, and IL-6, and also by TLR ligands, such as LPS and CpG-DNA (22). Several studies have demonstrated that SOCS1 is a negative regulator of LPS-induced macrophage activation and plays an essential role in suppression of systemic autoimmunity mediated by DCs (23–25). Thus, SOCS1 regulates not only adaptive immunity

*Laboratory of Immunoregulation and Vaccine Research, Tsukuba Primate Research Center, National Institute of Biomedical Innovation, Tsukuba, Ibaraki 305-0843, Japan; †Department of Cardiovascular Medicine, Majors of Medical Sciences, Graduate School of Comprehensive Human Sciences, University of Tsukuba, Tsukuba, Ibaraki 305-8575, Japan; ‡Department of Pathology and Matrix Biology, Mie University Graduate School of Medicine, Tsu, Mie 514-8507, Japan; §Mie University Matrix Biology Research Center, Mie University Graduate School of Medicine, Tsu, Mie 514-8507, Japan; ¶Division of Immunoregulation, Department of Molecular and Experimental Medicine, Mie University Graduate School of Medicine, Tsu, Mie 514-8507, Japan; ‖Department of Cardiology, National Center for Global Health and Medicine, Shinjuku, Tokyo 162-8655, Japan; and #Laboratory of Immune Signal, National Institute of Biomedical Innovation, Ibaragi, Osaka 565-0871, Japan

Received for publication December 13, 2011. Accepted for publication June 5, 2012.

This work was supported by Health Science Research grants from the Ministry of Health, Labor and Welfare of Japan and the Ministry of Education, Culture, Sports, Science and Technology of Japan.

Address correspondence and reprint requests to Dr. Yasuhiro Yasutomi, Laboratory of Immunoregulation and Vaccine Research, Tsukuba Primate Research Center, National Institute of Biomedical Innovation, 1-1 Hachimandai, Tsukuba, Ibaraki 305-0843, Japan. E-mail address: yasutomi@nibio.go.jp

The online version of this article contains supplemental material.

Abbreviations used in this article: BMDC, bone marrow-derived dendritic cell; DC, dendritic cell; dnSOCS1, dominant-negative suppressor of cytokine signaling 1; EAM, experimental autoimmune myocarditis; FS, fractional shortening; KO, knockout; LV, left ventricular; LVEDd, left ventricular end-diastolic dimension; LVESd, left ventricular end-systolic dimension; MyHC-α, cardiac myosin-specific peptide; pdnSOCS1, plasmid vector encoding dominant-negative suppressor of cytokine signaling 1; pSOCS1, plasmid vector encoding suppressor of cytokine signaling 1; QRT-PCR, quantitative real-time RT-PCR; SOCS, suppressor of cytokine signaling.

www.jimmunol.org/cgi/doi/10.4049/jimmunol.1103610

but also innate immunity by suppressing hyperactivation of macrophages and DCs.

In this study, we describe the therapeutic effect of SOCS1 DNA administration using plasmid DNA encoding SOCS1 for EAM. SOCS1 DNA therapy reduces myocarditis by regulating DC populations during EAM.

Materials and Methods

Animals

BALB/c mice and CB17.SCID mice were purchased from CLEA Japan. We used 5–7-wk-old male mice. All animals were cared for according to ethical guidelines approved by the Institutional Animal Care and Use Committee of the National Institute of Biomedical Innovation.

Immunization protocols

Mice were immunized with 100 μg cardiac myosin-specific peptide (MyHC-$\alpha_{614-629}$) Ac-RSLKLMATLFSTYASADR-OH (Toray Research Center) emulsified 1:1 in PBS/CFA (1 mg/ml; H37Ra; Sigma-Aldrich) on days 0 and 7 as described previously (12). For DC immunization, bone marrow-derived DCs (BMDCs) were generated as described (26). BMDCs were pulsed overnight with 10 μg/ml MyHC-α peptide and stimulated for another 4 h with 0.1 μg/ml LPS (Sigma-Aldrich) and 5 μg/ml anti-CD40 (BD Pharmingen) (15). Recipient mice received 2.5×10^5 pulsed and activated BMDCs i.p. on days 0, 2, and 4 and were killed 10 d after the first injection.

Plasmid construction and DNA transfection

Mouse SOCS1 cDNA and dominant-negative SOCS1 (dnSOCS1) cDNA were subcloned into the mammalian vector pcDNA3.1-myc/His(-) using oligonucleotide primers containing restriction sites for XhoI and EchoRI at the 5′ and 3′ ends, respectively. MyHC-α/CFA-immunized mice were injected i.p. with 100 μg of plasmid DNA in 200 μl PBS on days 0, 5, and 10. BMDC-transferred mice and $CD4^+$ T cell adoptive-transferred SCID mice were treated with plasmid DNA on days 0 and 5.

Histopathologic examination

Myocarditis severity was scored on H&E-stained sections using grades from 0–4: 0, no inflammation; 1, <25% of the heart section involved; 2, 25–50%; 3, 50–75%; and 4, >75%. To quantify the fibrotic area, ventricular sections were stained with Sirius Red. The fibrotic area was calculated as the sum of all areas stained positive for Sirius Red divided by the sum of all myocardial areas in each mouse. Two independent researchers scored the slides separately in a blinded manner.

Flow cytometry

Heart inflammatory cells were isolated and processed as described (15, 27). Cells were stained using fluorochrome-conjugated mouse-specific Abs against CD45, CD4, CD3e, CD44, CD62L, and CD40L (BD Biosciences). Samples were analyzed on an FACSCalibur cell sorter (BD Biosciences).

Measurements of cytokines and chemokines

Hearts were homogenized in media containing 2.5% FBS. Supernatants were collected after centrifugation and stored at −80°C. For in vitro stimulation assay of primary $CD4^+$ T cells, naive $CD4^+CD62L^+$ T cells were isolated from the spleens by MACS ($CD4^+CD62L^+$ T Cell Isolation Kit II; Miltenyi Biotec). A total of 1.5×10^7 $CD4^+CD62L^+$ cells were then stimulated with recombinant mouse IL-2 (R&D Systems) or recombinant mouse IL-12 (R&D Systems). Concentrations of cytokines and chemokines in the heart homogenates or culture supernatants were measured with Quantikine ELISA kits (R&D Systems).

Proliferative responses of T cells

Proliferation of T cells was assessed as previously described (28). Briefly, mice were immunized as described above, and the spleens collected on day 14. Cells were cultured with 5 μg/ml MyHC-α for 72 h and pulsed with 0.5 μCi [^{3}H]thymidine 8 h before being measured with a β counter. For in vitro stimulation assay of primary $CD4^+$ T cells, naive $CD4^+CD62L^+$ T cells were isolated from the spleens by MACS ($CD4^+CD62L^+$ T Cell Isolation Kit II; Miltenyi Biotec). A total of 10^5 $CD4^+CD62L^+$ cells were then stimulated with 5 μg/ml anti-CD3ε, 5 μg/ml anti-CD3ε, 1 μg/ml anti-CD28, 50 ng/ml PMA, and 500 ng/ml ionomycin or with 1 μg/ml Con A together with 0.25×10^5 DCs. Proliferative responses were assessed after 48 h in 2.5% RPMI 1640 medium by measurement of the [^{3}H]thymidine incorporation.

Western blot analysis

Total lysates from $CD4^+$ T cells or DCs were immunoblotted and probed with Abs directed against STAT1 (Santa Cruz Biotechnology) and p-STAT1 protein (Cell Signaling Technology). HRP-conjugated goat anti-rabbit IgG (Bio-Rad) was used to identify the binding sites of the primary Ab.

Adoptive transfer of T cells

Splenocytes were collected from diseased mice and cultured with 5 μg/ml MyHC-α for 48 h. A total of 5×10^6 $CD4^+$ T cells were purified by using anti-CD4 magnetic beads (Miltenyi Biotec) and injected i.p. into the SCID mice. The mice were killed 10 d after the injection.

Quantitative real-time RT-PCR

Total RNA was prepared using TRIzol reagent (Invitrogen) according to the manufacturer's instructions. cDNA was synthesized from 1 μg total RNA by reverse transcriptase (Takara). Quantitative real-time RT-PCR (QRT-PCR) analysis was performed with LightCycler (Roche Diagnostics). Primers for mouse *Socs1* were 5′-GTGGTTGTGGAGGGTGAGAT-3′ (sense) and 5′-CCTGAGAGGTGGGATGAGG-3′ (antisense). Primers for mouse *Hprt* were 5′-TCCTCCTCAGACCGCTTTT-3′ (sense) and 5′-CCTGGTTCATCATCGCTAATC-3′ (antisense). Data were normalized by the level of *Hprt* expression in each sample.

Echocardiography

Transthoracic echocardiography was performed on animals on day 35 by using a Prosound α6 with a 10-MHz transducer (Aloka). The left ventricular (LV) chamber dimensions were measured from the M-mode. Two independent investigators who conducted the echocardiography were unaware of the treatment status.

Statistical analysis

All data were expressed as means ± SEM. Statistical analyses were performed using the two-tailed *t* test or Mann–Whitney *U* test for experiments comparing two groups. The *p* values <0.05 were considered statistically significant.

Results

SOCS1 DNA administration inhibits the development of EAM

To examine the effect of in vivo gene delivery of *Socs1* on the pathogenesis of EAM, BALB/c mice were injected with a mammalian expression plasmid vector encoding SOCS1 (pSOCS1) during the course of EAM induction (Fig. 1A). QRT-PCR analysis revealed elevated expression of *Socs1* in the control EAM heart (Fig. 1B). Importantly, in the SOCS1 DNA-administered mice, *Socs1* was strongly expressed in the heart. By day 28, *Socs1* gene expression was significantly elevated in the pSOCS1-treated heart as compared with the controls (Supplemental Fig. 1). Gross cardiac enlargement and edema were reduced in mice with EAM that received pSOCS1 as compared with those in control empty plasmid DNA-administered EAM mice (Fig. 1C). The heart-to-body weight ratio in the pSOCS1-injected mice was significantly decreased as compared with that in the control plasmid-administered mice (Fig. 1D). The pSOCS1-injected EAM mice had a significantly lower myocarditis severity score and fewer infiltrating inflammatory cells than did the control plasmid-injected mice (Fig. 1E–G). The empty vector [pcDNA3.1-myc/His(-)] was used as the control and did not have any effects on EAM in our experiments (data not shown).

Recently, Hanada et al. (29) demonstrated that dnSOCS1, which has a point mutation (F59D) in a functionally critical kinase inhibitory region of SOCS1, strongly augmented cytokine-dependent JAK-STAT activation both in vivo and in vitro as an antagonist of SOCS1. We examined the effect of dnSOCS1 on the clinical course of EAM. Mice administered a plasmid vector

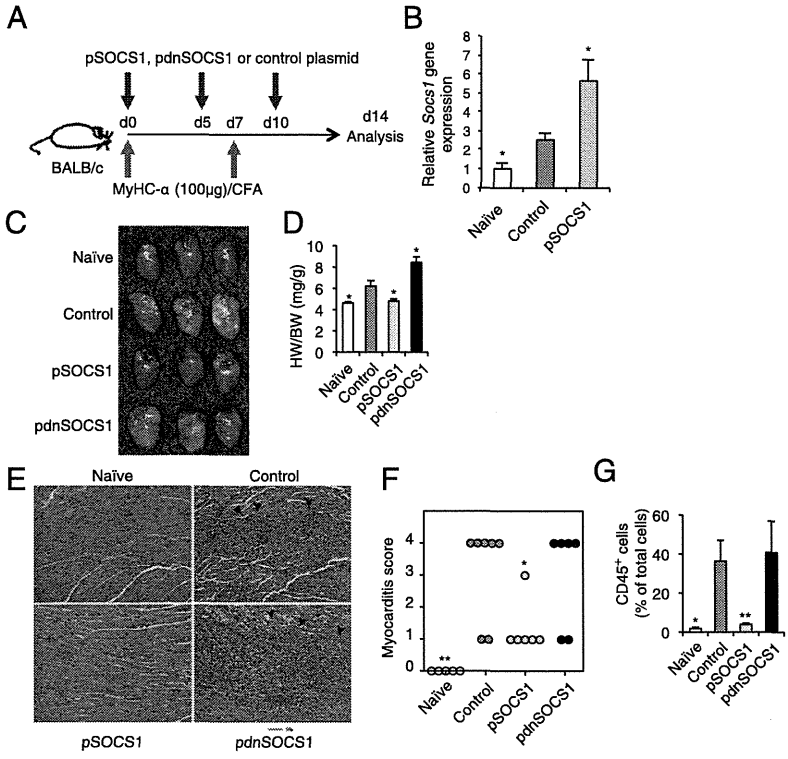

FIGURE 1. Amelioration of EAM and heart failure by SOCS1 DNA administration. (**A**) BALB/c mice were immunized twice, on days 0 and 7, with 100 μg of MyHC-α and treated with pSOCS1, pdnSOCS1, or control plasmid on days 0, 5, and 10. (**B**) QRT-PCR for the *Socs1* gene. RNA samples were obtained from hearts of immunized mice on day 14 and used as a template for QRT-PCR. Results represent the average gene induction in five independent heart samples. (**C**) Representative gross hearts (day 14) of naive and EAM mice treated with the indicated plasmid. (**D**) Heart-to-body weight ratios of naive and EAM mice with indicated treatment (n = 5 mice/group). (**E**) Representative H&E-stained sections of hearts from naive and immunized mice. Arrowheads indicate infiltrating cells. Scale bar, 50 μm. (**F**) Myocarditis severity in heart sections stained with H&E (n = 5–7 mice/group). (**G**) Flow cytometry analysis of $CD45^+$ heart infiltrates of naive and immunized mice (n = 5–7 mice/group). Data are representative of at least two independent experiments. Error bars represent means ± SEM. $*p < 0.05$, $**p < 0.01$ compared with control.

encoding dnSOCS1 (pdnSOCS1) showed augmentation of gross heart enlargement, edema, and heart-to-body weight ratio (Fig. 1C, 1D). However, the myocardial leukocyte infiltration and myocarditis scores were not significantly different between the pdnSOCS1- and control plasmid-administered mice (Fig. 1E–G).

To clarify the adverse effect of dnSOCS1 DNA administration on the development of EAM, we used mice immunized with a tithe amount (10 μg) of MyHC-α instead of the usual amount of peptide for EAM development (Fig. 2A). Those MyHC-α–immunized mice injected with the control plasmid or pSOCS1 did not develop myocarditis (Fig. 2B–F). However, immunized mice injected with pdnSOCS1 developed myocarditis with inflammatory infiltrates (Fig. 2B–F). Thus, administration of pSOCS1 is effective against the development of EAM, and the inhibition of SOCS1 by use of a SOCS1 antagonist adversely affects myocarditis.

SOCS1 DNA administration prevents progression of heart failure and fibrosis after myocarditis

Some patients diagnosed with myocarditis after viral, bacterial, or protozoal infection develop heart failure (2). On day 35 of the present experiment, mice immunized with MyHC-α showed increased LV end-diastolic dimensions (LVEDd) and LV end-systolic dimensions (LVESd) and decreased fractional shortening (FS); however, pSOCS1-injected mice showed almost normal chamber size and LV function (Fig. 3A, 3B). In contrast, LV dysfunction and chamber dilatation in pdnSOCS1-administered mice were manifested as significant increases in LVEDd and LVESd and decrease in FS (Fig. 3A, 3B). In these EAM models, on day 35, hearts from myocarditis mice showed interstitial fibrosis without active leukocyte infiltration. The fibrotic area in mice administered pSOCS1 was significantly smaller than that in control plasmid-injected mice (Fig. 3C, 3D). Although pdnSOCS1-injected mice developed severe cardiac fibrosis, the difference between the fibrotic areas in pdnSOCS1- and control plasmid-injected mice was not statistically significant (Fig. 3C, 3D). These inhibitory effects of pSOCS1 on the development of fibrosis and heart failure were considered to be the result of inhibition of myocardial inflammation because myocarditis developed mice injected with pSOCS1 on day 14, 21, and 28 did not show inhibitory effects on fibrosis and heart failure (data not shown).

Cardiac myosin-specific $CD4^+$ T cell response and cytokine production

Autoimmune myocarditis is a $CD4^+$ T cell-mediated disease (7, 15). Proliferative responses of $CD4^+$ T cells after in vitro restimulation with MyHC-α were not clearly seen in pSOCS1-injected mice; however, the proliferation of $CD4^+$ T cells from pdnSOCS1-injected mice was enhanced (Fig. 4A). Production of IL-2, IL-6, IL-10, IL-17, IL-22, IFN-γ, TNF-α, CCL2, CCL3, CCL5, CCL17, and CXCL10 by $CD4^+$ T cells from EAM mice was enhanced by in vitro restimulation with the MyHC-α epitope peptide. This cardiac-Ag–specific cytokine production by $CD4^+$ T cells was decreased in the supernatants of in vitro MyHC-α–restimulated $CD4^+$ T cells from pSOCS1-administered mice but

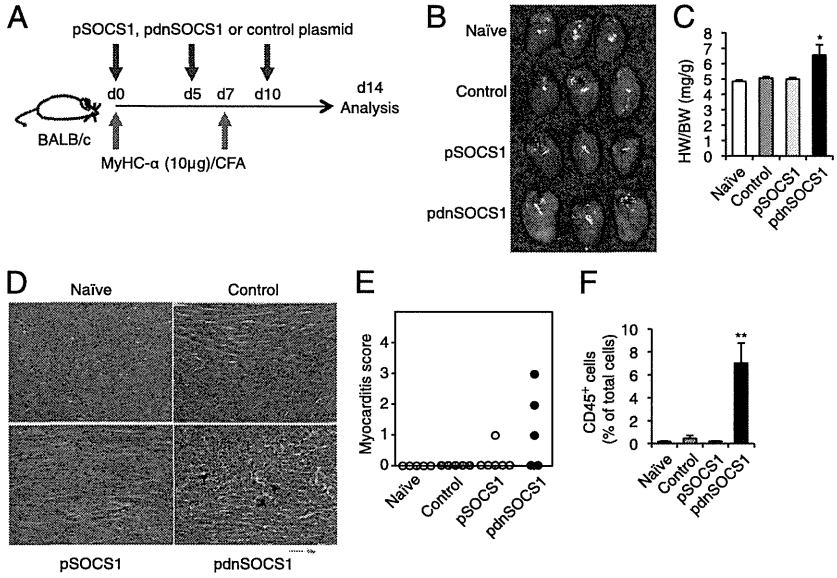

FIGURE 2. Increased susceptibility to EAM induced by inhibition of SOCS1. (**A**) Mice were immunized twice, on days 0 and 7, with 10 μg of MyHC-α emulsified 1:1 in PBS/CFA and treated with pSOCS1, pdnSOCS1, or control plasmid on days 0, 5, and 10. (**B**) Representative gross hearts (day 14) of naive and 10 μg of MyHC-α–immunized mice treated with the indicated plasmid. (**C**) Heart-to-body weight ratios of naive and immunized mice (n = 5 to 6 mice/group). (**D**) Representative H&E-stained sections of hearts from naive and immunized mice. Arrowheads indicate infiltrating cells. Scale bar, 50 μm. (**E**) Myocarditis severity in heart sections stained with H&E (n = 5 to 6 mice/group). (**F**) Flow cytometry analysis of $CD45^+$ heart infiltrates of naive and immunized mice (n = 5 mice/group). Data are representative of at least two independent experiments. Error bars represent means ± SEM. $*p < 0.05$, $**p < 0.01$ compared with control.

was increased in the supernatants of these cells from pdnSOCS1-administered mice (Fig. 4B). In contrast, cardiac-Ag–specific production of IL-1β, IL-10, and CXCL1 was not detected in the culture supernatants of in vitro-restimulated $CD4^+$ T cells from control plasmid-, pSOCS1-, or pdnSOCS1-injected mice (data not shown). Taken together, these results indicate that SOCS1 DNA

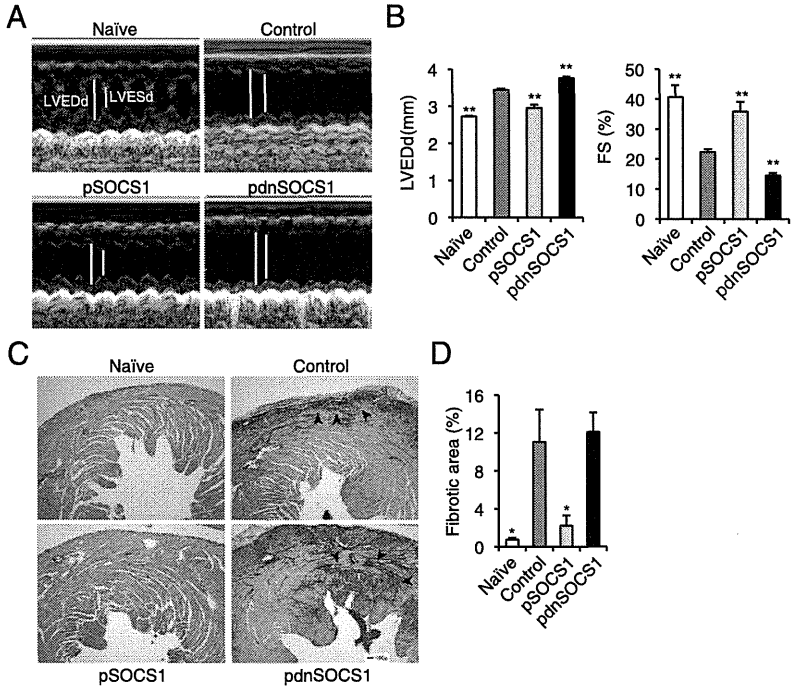

FIGURE 3. SOCS1 DNA administration prevents progression to heart failure. (**A** and **B**) Echocardiography was performed on naive and immunized mice on day 35. (A) Representative M-mode echocardiograms. Bars indicate LVESd and LVEDd. Bar graphs (B) represent LVEDd and percentage of FS from the indicated animals (n = 9 mice/group). The percentage FS was calculated according to the following formula: FS (%) = (LVEDd − LVESd)/LVEDd. (**C** and **D**) Heart tissue sections were stained with Sirius Red and analyzed for fibrosis at day 35. Representative Sirius Red-stained sections of hearts. Scale bar, 50 μm. (C) Arrowheads indicate fibrotic area. (D) The degree of fibrosis was calculated as the percentage of the fibrotic area in relation to the total heart area (n = 5 mice/group). Data are representative of at least two independent experiments. Error bars represent means ± SEM. $*p < 0.05$, $**p < 0.01$ compared with control.

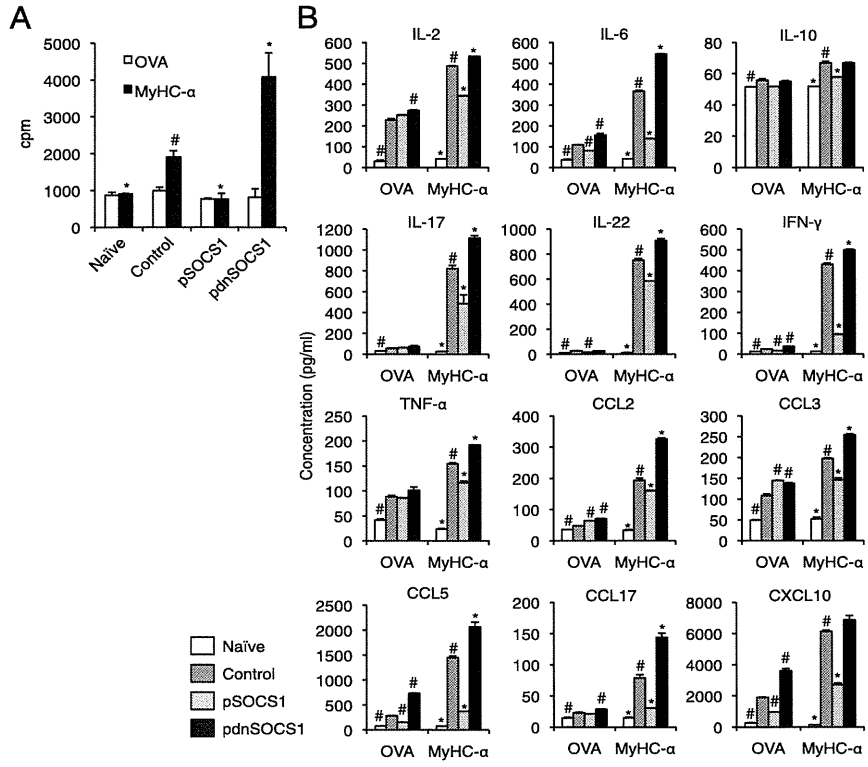

FIGURE 4. Impaired expansion of heart-specific CD4$^+$ T cells in pSOCS1-treated mice. (**A**) Splenocytes were isolated from naive and EAM mice treated with pSOCS1, pdnSOCS1, or control plasmid on day 14 and restimulated in vitro with MyHC-α or OVA peptide for 72 h. Proliferation was assessed by measurement of [^{3}H]thymidine incorporation. Data represent means ± SEM of triplicates from one of three independent experiments. (**B**) Cytokines and chemokines in the culture supernatants of splenocytes were measured by ELISA after 48 h of restimulation with MyHC-α or OVA peptide. Data are expressed as mean ± SEM from triplicate culture wells. Results of one of two representative experiments are shown. $^*p < 0.05$ compared with MyHC-α–stimulated control, $^\#p < 0.05$ compared with OVA-stimulated control.

delivery inhibits the activation of myosin-specific CD4$^+$ T cells and strongly suggest that impaired CD4$^+$ Th cell function prevents EAM development in pSOCS1-injected mice after immunization with cardiac self-Ag.

To evaluate whether pSOCS1 administration affects Ag-specific CD4$^+$ T cell function in other models, we injected plasmid DNA into an autoimmune gastritis model and an OVA-immunized model. In the autoimmune gastritis model, gastric-Ag–specific production of IL-2, IL-6, IL-13, IL-17, IL-22, IFN-γ, TNF-α, CCL2, CCL5, CCL17, and CXCL10 by CD4$^+$ T cells was decreased in pSOCS1-administered mice but increased in pdnSOCS1-administered mice (Supplemental Fig. 2). Lower amounts of cytokines (including IL-2, IL-6, IL-13, IFN-γ, TNF-α, CCL2, CCL3, CCL5, CCL17, and CXCL10) were also produced in CD4$^+$ T cells from pSOCS1-injected OVA-immunized mice (Supplemental Fig. 3). These results suggest that pSOCS1 administration may suppress Ag-specific CD4$^+$ T cell activation in various autoimmune diseases and foreign body infections.

SOCS1 DNA administration inhibits the production of proinflammatory cytokines and CD4$^+$ T cell differentiation in the heart

We also examined whether SOCS1 DNA administration has an effect on cytokine and chemokine milieu in the heart. On day 14 after MyHC-α immunization, heart homogenates from pSOCS1-injected mice had significantly decreased amounts of proinflammatory cytokines, including IL-1β and IL-6, and of myelotropic chemokines, including CCL5, CXCL1, and CXCL10 (Fig. 5A). In contrast, hearts from mice injected with pdnSOCS1 showed greatly increased amounts of proinflammatory cytokines and chemokines (Fig. 5A). SOCS1 protein has been shown to regulate T cell differentiation (17, 18). To determine the differentiation of CD4$^+$ T cells during EAM, we examined the heart-infiltrating CD4$^+$ T cell populations by FACS analysis. Activated CD4$^+$ T cells (CD4$^+$CD40L$^+$) and effector memory CD4$^+$ T cells (CD44$^+$CD62L$^-$) were reduced in the pSOCS1-injected mice (Fig. 5B). Thus, protection from EAM in pSOCS1-administered mice is associated with abrogation of proinflammatory cytokines, chemokines, and CD4$^+$ T cell differentiation in the heart.

SOCS1 DNA injection does not have a direct suppressive effect on CD4$^+$ T cell activation

To gain new insights into the mechanism of protection from myocarditis, we investigated whether pSOCS1 therapy directly affects CD4$^+$ T cell activation. Naive T cells (CD4$^+$CD62L$^+$ cells) were isolated from non-EAM mice injected with pSOCS1, pdnSOCS1, or control plasmid, and their primary responses to various stimuli were compared (Fig. 6A). As shown in Fig. 6B, there were no differences in IFN-γ–induced STAT1 activation among these CD4$^+$ T cells. There were also no differences in primary responses to stimulation with anti-CD3ε, anti-CD3ε/anti-CD28, PMA/ionomycin, or Con A presented by mitomycin C-treated wild-type DCs among pSOCS1-, pdnSOCS1-, and control plasmid-treated CD4$^+$ T cells (Fig. 6C). Chong et al. (30) demonstrated that SOCS1-deficient T cells produced substantially greater levels of IFN-γ in response to IL-2 or IL-12. From these findings, we assessed the production of IFN-γ from CD4$^+$ T cells by using the same experiments. In the culture supernatants of

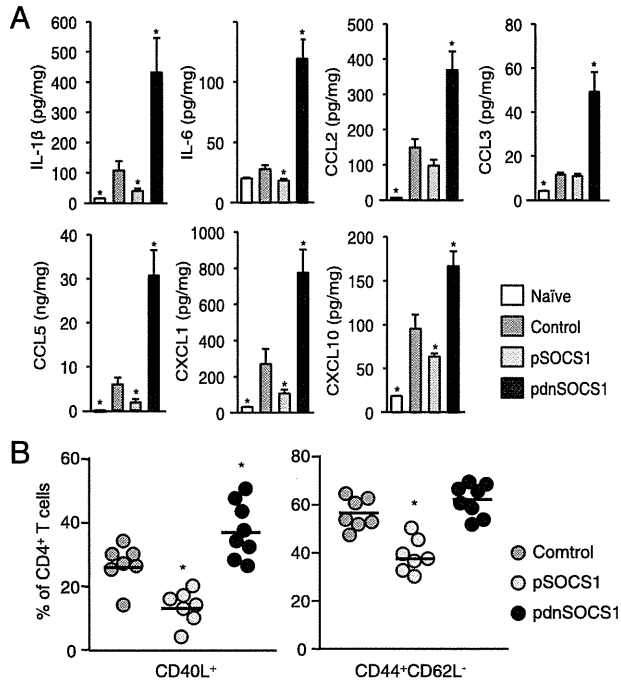

FIGURE 5. Cytokine and chemokine responses and $CD4^+$ T cell differentiation in the heart. (**A**) Myocardial tissues were homogenated and processed by ELISA to detect cytokines and chemokines on day 14. Bar graphs show group means ± SEM of 8–16 mice/group. Results of one of three representative experiments are shown. (**B**) Heart-infiltrating cells were isolated from EAM mice treated with indicated plasmid DNA. Cells were stained for CD4, CD40L, CD44, and CD62L. CD44 and CD62L expression are based on gates set from total $CD4^+$ T cells. Bar graphs show group means ± SEM of 5–9 mice/group. Data are representative of two independent experiments. $*p < 0.05$ compared with control.

$CD4^+$ T cells stimulated with IL-2 or IL-12, there were also no differences in IFN-γ production (Fig. 6D). These results indicate that in vivo administration of pSOCS1 does not directly affect $CD4^+$ T cell activation.

In vivo SOCS1 DNA administration inhibits DC function

Although $CD4^+$ T cell differentiation was inhibited in pSOCS1-treated mice (Fig. 5B), our results suggested that in vivo *Socs1* gene administration has no direct effect on $CD4^+$ T cell activation (Fig. 6). We therefore investigated whether in vivo pSOCS1 administration inhibits the function of Ag-presenting DCs by stimulation through the TLR pathway. DCs from mice administered pSOCS1, pdnSOCS1, or control plasmid were stimulated with LPS for 24 h (Fig. 7A). STAT1 phosphorylation was attenuated in DCs from pSOCS1-injected mice and enhanced in DCs from pdnSOCS1-injected mice (Fig. 7B). The production of proinflammatory cytokines, including IL-6, TNF-α, and IFN-γ, was inhibited in DCs from pSOCS1-injected mice and enhanced in DCs from pdnSOCS1-injected mice (Fig. 7C). These results indicate that in vivo administration of *Socs1* affects DC function. In the current study, the cardiac-Ag–specific proliferative response and cytokine production of $CD4^+$ T cells were inhibited in pSOCS1-injected EAM mice (Fig. 4). We next assessed the functional capability of DCs to prime and expand autoreactive $CD4^+$ T cells from mice injected with each plasmid as a measure of Ag-specific proliferative responses of $CD4^+$ T cells from MyHC-α–immunized mice. Myosin-specific $CD4^+$ T cells were cocultured with MyHC-α–pulsed DCs from pSOCS1-, pdnSOCS1-, and control plasmid-treated mice (Fig. 7D). Interestingly, the proliferative responses of $CD4^+$ T cells cocultured with DCs from pSOCS1-treated mice were much weaker than those of cells cultured with DCs from control plasmid-treated mice, and these proliferative responses of $CD4^+$ T cells were enhanced by coculturing with DCs from pdnSOCS1-administered mice (Fig. 7E). These results suggest that in vivo gene delivery of *Socs1* suppresses the functional capability of DCs to prime and expand autoreactive $CD4^+$ T cells.

SOCS1 DNA administration inhibits the development of myocarditis induced by cardiac myosin peptide-loaded BMDC transfer but not by $CD4^+$ T cell transfer

Functionally interposed SOCS1 is induced in various cell populations, including leukocytes, vascular cells, and cardiomyocytes (18, 31, 32). A mouse model of EAM was established by cell transfer using peptide-pulsed DCs or cardiac epitope-specific $CD4^+$ T cells (7, 14). The effects of pSOCS1 administration in mice transferred with $CD4^+$ T cells from mice with EAM were assessed. pSOCS1, pdnSOCS1, or control plasmid was injected into mice transferred with cardiac myosin-specific $CD4^+$ T cells (Fig. 8A). All mice transferred with $CD4^+$ T cells developed myocarditis, and no therapeutic effects were seen in pSOCS1-injected mice (Fig. 8B–D). Furthermore, pdnSOCS1 administration showed no adverse effect on the status of myocarditis induced by $CD4^+$ T cell transfer (Fig. 8B–D). These findings suggest that systemic injection of pSOCS1 is not effective for inhibition of autoreactive $CD4^+$ T cell activation and recruitment to the heart during myocarditis development. Next, we administered pSOCS1, pdnSOCS1, or control plasmid into mice transferred with MyHC-α–loaded BMDCs (Fig. 8E). Interestingly, pSOCS1 injection inhibited the development of myocarditis after MyHC-α–loaded BMDC transfer, and myocarditis deteriorated after administration of pdnSOCS1 (Fig. 8F–H). These results indicate that the therapeutic effects of SOCS1 DNA administration on EAM contribute to professional APCs such as DCs and also provide evidence for the potential utility of SOCS1 DNA inoculation as an approach to gene therapy for myocarditis.

Discussion

There have been no effective fundamental therapies for acute myocarditis; therefore, supportive care for LV dysfunction is the first line of treatment. Because patients generally present days to weeks after the initial viral infection, antiviral therapy has limited applicability in patients with acute viral myocarditis. The long-term sequelae of viral myocarditis appear to be related to abnormal cellular and humoral immunity; therefore, many clinicians believe that immunosuppression is beneficial for myocarditis treatment (2). In this study, we showed that administration of SOCS1 DNA is effective for inhibiting the development of EAM in BALB/c mice, suggesting a novel immunotherapy for myocarditis. To our knowledge, this is the first report showing that gene delivery of *Socs1* prevents autoimmune disease.

Animal models have greatly advanced our knowledge of the pathogenesis of myocarditis and inflammatory cardiomyopathy. Infection of BALB/c mice with either Coxsackievirus or murine CMV results in the development of acute myocarditis from days 7–14 postinfection that is characterized by myocyte damage due to viral cytotoxicity, and the infectious virus cannot be detected past day 14 of the infection (7). After elimination of viruses, mice showed autoimmune myocarditis, which is associated with mononuclear infiltration of the myocardium and production of autoantibodies to cardiac myosin (7), similar to the pathogenesis of autoimmune myocarditis in humans (3, 4, 33). These autoim-

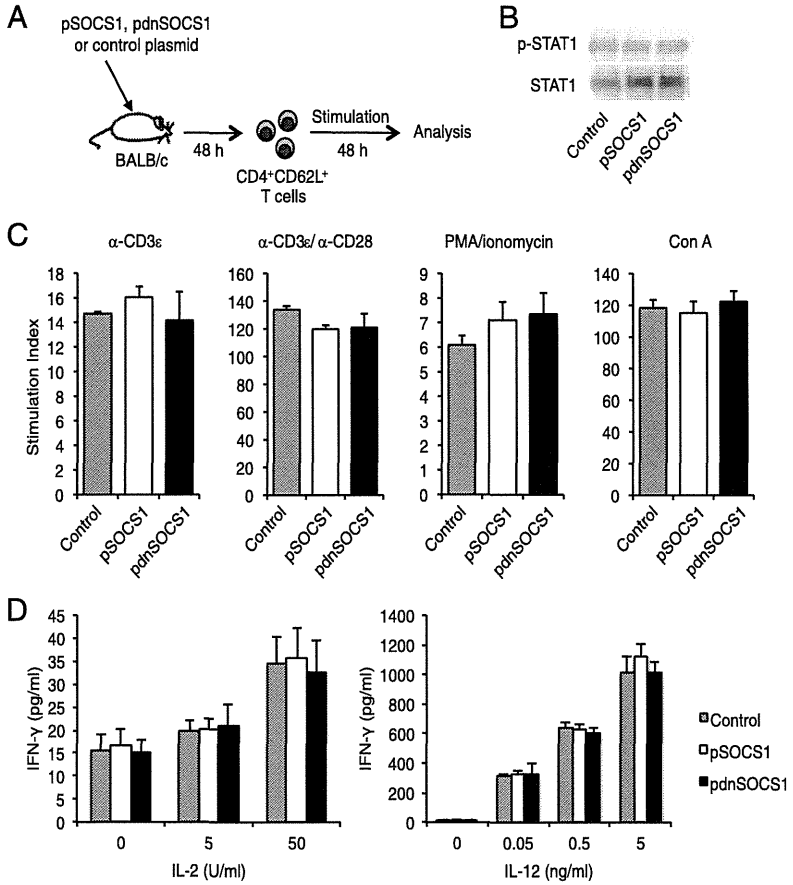

FIGURE 6. Primary responses of $CD4^+$ T cells from pSOCS1-, pdnSOCS1-, and control plasmid-treated mice. (**A**) $CD4^+CD62L^+$ T cells from mice injected with pSOCS1, pdnSOCS1, or control plasmid were stimulated with IFN-γ, anti-CD3ε, anti-CD3ε, anti-CD28, PMA/ionomycin, and Con A in the presence of wild-type DCs, IL-2, or IL-12. (**B**) STAT1 phosphorylation of $CD4^+$ T cells after IFN-γ treatment (10 ng/ml) was assessed by Western blotting. (**C**) T cell proliferation was measured after 48 h of culture. (**D**) IFN-γ in the culture supernatants was measured by ELISA. Values are expressed as means ± SEM of triplicate culture wells. Results of one of at least two representative experiments are shown.

mune responses are thought to be elicited by two mechanisms. One is molecular mimicry: responses to microbial Ags could result in the activation of T cells that are cross-reactive with self-Ags. Another possibility is bystander activation of autoreactive cells. APCs that have become activated in the inflammatory milieu of a pathogenic infection can stimulate the activation and proliferation of autoreactive T or B cells in a process known as bystander activation (reviewed in Ref. 34). Thus, immune responses to myocytes involving various innate and adaptive immune pathways were recognized during myocarditis development. The cardiac myosin peptide-immunized mouse EAM model reflects human autoimmune myocarditis and heart failure after elimination of infectious pathogens.

Recent studies have indicated that various microbes use the host's SOCS proteins for manipulating cytokine receptor signaling as one of the strategies to evade immune responses (35, 36). Coxsackievirus usually infects cardiomyocytes and induces the expression of SOCS1 and SOCS3 in cardiomyocytes, which can result in evasion of immune responses and facilitation of virus replication by inhibition of JAK–STAT signaling (32, 37). These findings indicate that it may be harmful to administer SOCS1 DNA in the acute phase of infectious myocarditis because it may augment viral replication by inhibition of IFN signaling. The effect of SOCS1 transduction on viral myocarditis has been examined by Yasukawa et al. (32). The SOCS1-transgenic mice infected with CVB3 showed increased myocardial injury, virus replication, and mortality. In contrast, they also showed that SOCS1 inhibition in the heart through adeno-associated virus-mediated expression of dnSOCS1 increased resistance to the acute cardiac injury caused by CVB3 infection. These results were acceptable because SOCS proteins have emerged as frequent targets of viral exploitation. Furthermore, when administrating JAK inhibitors, such as SOCS, active serious infections should have been resolved before the start of treatment. It is considered to be inappropriate to use JAK inhibitors for a person with infectious disease or their possibility with consideration for complication of infection (38–40). In contrast, the overactive autoimmune responses triggered by microbial pathogens can persist after elimination of infectious pathogens (7). Therefore, we examined the efficacy of SOCS1 transfection by using EAM induced by cardiac autoantigen immunization in the absence of viral infection. In the current study, we clearly showed the efficacy of *Socs1* gene transfer as an immunosuppressive therapy for myocarditis under infectious pathogen-free conditions in an EAM mice model. The results of a recent randomized, double-blind, placebo-controlled study showed that immunosuppressive therapy, including prednisone and azathioprine, was effective in patients with myocarditis and inflammatory cardiomyopathy and without evidence of the myocardial viral genome (41). These findings indicate that *Socs1* gene transfer can be effective to treat some clinical